arXiv:1511.05930v1 [astro-ph.GA] 18 Nov 2015

COMPARISON OF HIPPARCOS TRIGONOMETRIC AND MOUNT WILSON SPECTROSCOPIC PARALLAXES FOR 90 SUBGIANTS THAT DEFINED THE CLASS IN 1935

Allan Sandage,[1,2] Rachael L. Beaton,[1,3]
and
Steven R. Majewski[3]

ABSTRACT

A history is given of the discovery between 1914 and 1935 of stars of intermediate luminosity between giants and dwarfs with spectral types between G0 to K3. The Mount Wilson spectroscopists identified about 90 such stars in their 1935 summary paper of spectroscopic absolute magnitudes for 4179 stars. Called "subgiants" by Strömberg, these 90 stars defined the group at the time. The position of the Mount Wilson subgiants in the HR diagram caused difficulties in comparisons of high weight trigonometric parallaxes being measured in the 1930s and with Russell's prevailing evolution proposal, and critics questioned the reality of the Mount Wilson subgiants. To show that the 1935 Mount Wilson subgiants are real, we compare, star-by-star, the Mount Wilson spectroscopic absolute magnitudes of the 90 stars defining their sample against those absolute magnitudes derived from *Hipparcos* trigonometric parallaxes. We address concerns over biases in the Mount Wilson calibration sample and biases created by the adopted methodology for calibration. Historically, these concerns were sufficient to discredit the discovery of subgiants in the Mount Wilson sample. However, as shown here, the majority of the Mount Wilson stars identified as subgiants that also have reliable *Hipparcos* trigonometric parallaxes do lie among the subgiant sequence in the *Hipparcos* HR diagram. Moreover, no significant offset is seen between the M_V brightnesses derived from the Mount Wilson spectroscopic parallaxes and the M_V values derived from *Hipparcos* trigonometric parallaxes with $\sigma_\pi/\pi < 0.10$, which confirms in an impressive manner the efficacy of the original Mount Wilson assessments. The existence of subgiants proved that Russell's contraction proposal for stellar evolution from giants to the main sequence was incorrect. Instead, Gamow's 1944 unpublished conjecture that subgiants are post main-sequence stars just having left the main sequence was very nearly correct but was a decade before its time.

Subject headings: history and philosophy of astronomy – astronomical databases – stars: evolution – stars: subgiants – stars: fundamental parameters (classification, colors, luminosities)

1. Introduction

Often, in events leading to the beginning of a new field within science, there appears an observation or experiment, not understood at the time, that in the clarity of hindsight opened the field. There are many such episodes. A famous one in physics is the observation of at least 400 years ago that two bodies of different weights, when released from a height, reach the ground at the same time. This eventually lead to the general theory of relativity.

In astronomy, the initial discovery of subgiant

[1]The Observatories of the Carnegie Institution of Washington, 813 Santa Barbara Street, Pasadena, CA 91101

[2]deceased

[3]Department of Astronomy, University of Virginia, Charlottesville, VA 22904-4325 (rlb9n, srm4n@virginia.edu)

stars is such an episode. Subgiant stars are intermediate in luminosity in the HR diagram between the main-sequence dwarfs and the giants near $M_V = +0.5$. The subgiants occur at absolute magnitudes between M_V of +2 to +4 and spectral types between G0 and K3. Had they been fully understood from hints of their existence in the 1920s and their definitive discovery by Strömberg (1930) in his absolute magnitude calibration, the path to an understanding of stellar evolution might have been hastened.

The purpose of this paper is to recount the discovery of subgiants and to point out the difficulty that their existence posed for Russell's early theory of stellar evolution. We then address the concern of early doubters of their existence, but show that Strömberg's 1930 subgiants were real by comparing the Mount Wilson spectroscopic parallaxes of Adams et al. (1935) with modern *Hipparcos* trigonometric parallaxes for the ∼90 stars that defined the stellar class in 1935.

The plan of the paper is this. A history of the discovery of subgiants from 1917 to 1955 is given in the next subsection (Section 1.1). This is an extension of the very brief account given in Sandage et al. (2003, hereafter SLV03) The dilemma of the existence of subgiants for Russell's proposal (Russell 1914, 1925b,a) about the direction of stellar evolution and Gamow's conjecture for a solution is discussed in Section 2.

Section 3 is an account of the 1957 Vatican conference where the HR diagram of 25 subgiants with trigonometric parallaxes greater than $0''.052$ was discussed. The dilemma posed at that conference that field subgiants exist fainter than those in M67 is solved in Section 3.2 with an account of the discovery of the true ages of the old open clusters NGC 188 and NGC 6791.

In Section 4, the spectroscopic parallax technique is introduced and *Hipparcos* trigonometric absolute magnitudes are compared with the 1935 Mount Wilson spectroscopic magnitudes of the ∼90 proposed Mount Wilson subgiants. In Section 5, the biases in the Adams et al. (1935) dataset are isolated and properly removed from the data, to address and quantify the historical criticisms that challenged and colored perceptions of the veracity of the Mount Wilson spectroscopic dataset. Section 6 is a summary of the work presented here.

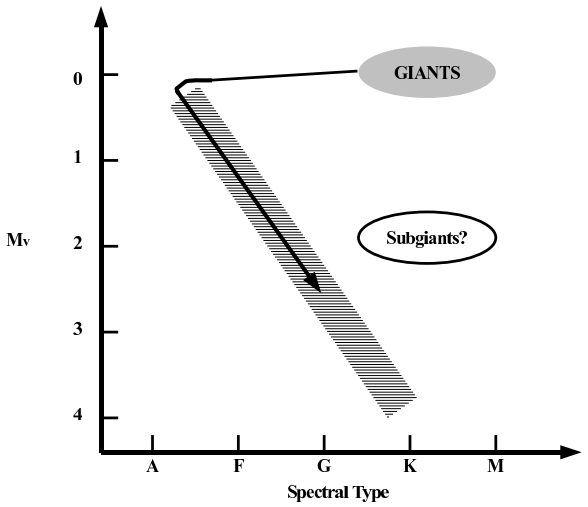

Fig. 1.— A schematic representation of Russell's evolutionary proposal for populating the main sequence by contraction of the giants and subsequent evolution down the main sequence at nearly constant radius after the main sequence stars become "rigid." The subgiants could not be accommodated by this contraction scenario. The position of the subgiants is adapted from the position of the subgiants in A35 (their Figure 1).

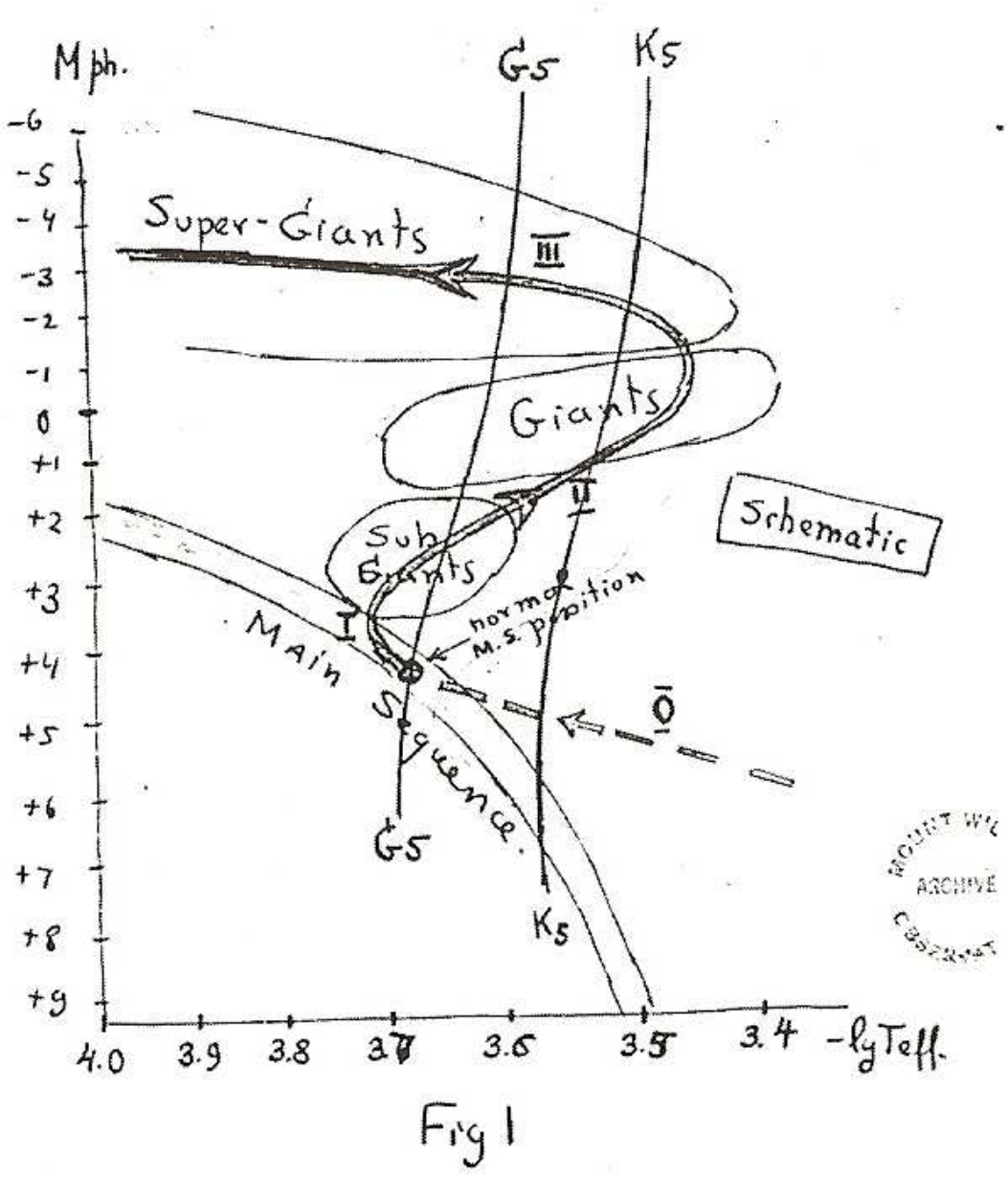

Fig. 2.— Gamow's unpublished conjecture from a letter to Adams on March 8, 1944 of evolution off the main sequence, through the subgiants, and then to the giants. This figure is reproduced from the Adams papers archive at the Huntington Library, San Marino, CA. A more accessible secondary source is DeVorkin (2006).

1.1. The Discovery

Following the invention of the method of measuring absolute magnitudes from stellar spectra by Adams & Kohlschütter (1914), Adams & Joy (1917) published their first long list of absolute magnitudes for 500 stars of spectral classes from F0 to M. The distribution of absolute magnitudes for various intervals of spectral type clearly showed the separation of giants and dwarfs, discovered by Hertzsprung (1905, 1907) and Russell (1914), but also showed a very few stars near $M_V = +2$ in the spectral interval from G0 to K3. The result is well shown in the distribution of Adams & Kohlschütter (1914). A matrix representation of their 500 star sample was set out by Adams & Joy (1922) three years later, reproduced for easier access in Sandage (2004, hereafter S04, Figure 15.6). This representation clearly illustrated how very few of these intermediate luminosity stars were included in the magnitude-limited sample of Adams & Joy (1917) — so few that one could question the reliability of their existence. However, Curtis (1922) had summarized all spectroscopic absolute magnitudes known at the time, and again, with imagination, one could make out a continuum distribution of absolute magnitudes between $M_V = +0.5$ and $+5$ for spectral types G5 and K0 (S04, Figure 15.5), yet the case for the existence of subgiants remained far from definitive.

Subgiants were also consistently appearing in studies of a different kind where absolute magnitudes were estimated by independent methods. The method of "proper motion statistical parallaxes" had been invented by Jacobus C. Kapteyn and Arnold Kohlschütter in application to K stars, but remained unpublished until its application to spectroscopic parallaxes was realized by Adams & Kohlschütter (1914). It relied on the size of the proper motion for "normal" stars, assuming that, statistically, in a large group of such stars, those with smaller proper motions were at larger distances. Luyten (1922) used the method with 4446 stars of known proper motion and showed in a matrix, much like that used by Adams & Joy (1922), that a continuum exists for stars of this type in the HR diagram between giants and dwarfs for spectral types G0 to K3. But again, no such continuum exists later than K3. Still, the number of such stars was minuscule

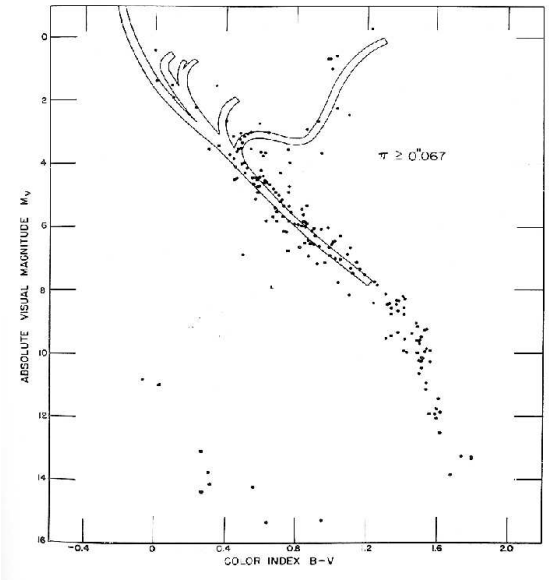

Fig. 3.— The HR diagram for stars within 20 parsecs of the Sun with relatively high weight trigonometric parallaxes known in 1957. Nine subgiants are fainter than the M67 subgiants, contrary to the expectation of the Vatican Conference, which raised questions of their reliability. Diagram from Sandage (1958b, his Fig. 3, p. 295).

and was generally ignored. The work with the so called "reduced proper motions" was repeated by Lundmark (1932), again using more than 4000 stars.

The final list of the Mount Wilson spectroscopic parallaxes and the resulting HR diagram derived was published in the famous summary paper by Adams, Joy, Humason and Brayton in 1935. In Adams et al. (1935, A35 hereafter), the subgiant sequence was unmistakable between G2 and K3 and at $\langle M_V \rangle = +2.5$, based on the statistical parallax calibrations of Strömberg (1930, 1932, 1936, see S04, Figs. 20.2, 20.3). Adams et al. wrote, "The existence of a group of stars of types G and K somewhat fainter than normal giants has been indicated by the statistical studies of Strömberg (1930, 1932). Although these stars may not be entirely separated from the giants in absolute magnitude, there is some spectroscopic evidence to support the suggestion."

During the later part of this Mount Wilson activity (1920-1935), such stars began appearing in lists of high weight trigonometric parallaxes and their existence could not be denied. By 1936, six extreme subgiants with large trigonometric parallaxes could be said to define a subgiant sequence independently of spectroscopic parallaxes. These were μ Her (type G5, trigonometric parallax = $0''.119$, $M_V = +3.75$); δ Eri (K0, $0''.111$, +3.68); 31 Aql (G8, $0''.059$, + 3.97); β Aql (G8, $0''.073$, +2.83); γ Cep (K1, $0''.072$, +2.223); and η Cep ($0''.070$, K0, +2.68).[1] The first three are fainter than the others by more than a magnitude, which shows the rather large intrinsic dispersion for the class. In the modern development of the *Hipparcos* HR diagram, this intrinsic spread is seen to be about 3 magnitudes (Perryman et al. 1995; Kovalevsky 1998).

In a historical and singular paper, Morgan (1937) acknowledges the existence of subgiants, calculating the surface gravity of β Aql, η Cep, and γ Cep — the stars defining the subgiant class at that time — to be intermediate between the surface gravities of giants and dwarfs. It is also in this paper that W. W. Morgan sets out the case for abandoning the assignment of absolute magnitudes to the Mount Wilson spectroscopic two dimensional classifications, and replacing them by a continuum of numbers ranging from -9 to $+21$. The numerical continuum, while ultimately related to the absolute magnitudes of the Mount Wilson system, was uncalibrated and represented the raw line ratios measured from the spectra, although intent was expressed to calibrate these values to absolute magnitudes at a later time.

This continuum of numbers was, eventually, replaced in the spectroscopic atlas of Morgan et al. (1943, hereafter MKK) with discrete boxes called luminosity classes, defining the MKK two dimensional system that discards the original Mount Wilson continuum system and replaces it by a digitized system with large classification boxes. In the 1943 MKK Atlas, the subgiant class was defined by the three stars used by Morgan (1937) to which μ Her and δ Eri were added. These five stars are among the "about 90 [stars] of types G and K somewhat fainter than normal giants" referred to by A35. The Yerkes subgiant class was designated as luminosity class IV and called subgiants following the name first given by Gustaf Strömberg.

By 1955, Eggen could discuss a group of 20 bright subgiants, some of which have companions permitting calculation of their masses. The result was that the mean mass is near 1.2 $M_\odot$, consistent with the expectation that the stars in Eggen's 1955 list are "evolving either from or toward the main sequence, near $M_V = +3.0$." Eggen (1955) showed that most of his 20 stars are within the borders of the subgiant sequence in the old open cluster M67 defined by Johnson (1954), although five are fainter (λ Aur, β Hyi, μ Her, 31 Aql, and δ Eri). Johnson had set up a photoelectric sequence in M67 in preparation for a complete photographic durchmusterung (Johnson & Sandage 1955), but had published his sequence before the photographic work was complete. In 1955, it was not clear how the subgiants tied onto the main sequence, a vital aspect that was sought but not clarified from previous work. Eggen's list of 20 subgiants are among those of A35 given in Table 2.1 here.

By 1957, Eggen produced a color-magnitude diagram (Fig. 1 in Eggen 1957) that clearly tied the few subgiants in a sample of 275 field stars brighter than $M_V = 5.0$ to the M67 main sequence and to the base of the first ascent giants. Eggen's Fig-

[1] Values for the trigonometric parallax and M_V are those from that era, but these values are remarkably close to those found by the *Hipparcos* satellite.

ure 1 was mentioned by Walter Baade at the 1957 Vatican Conference (Baade 1958). At that conference one of us could produce a list of 25 subgiants with high weight trigonometric parallaxes that defined the subgiant sequence discussed there (Sandage 1958b, reproduced here as Figure 3).

After the conference, two massive papers on motions, masses, and luminosities of bright local field subgiants by Eggen (1960, 1964) completed the discovery phase for the subgiant luminosity class.

2. The Dilemma for Russell's Evolution Proposal; Gamow's Supposition

2.1. Russell's Dilemma

As stated in the Introduction, in his discovery paper and thereafter, Russell (1914, 1925b,a) proposed that stars evolve by contraction from an initial giant phase, whereupon reaching the main-sequence dwarfs they become "rigid," stopping the contraction. Although in the 1920s, Sir Arthur Eddington had proved that main-sequence stars do not become "rigid" (main-sequence stars have a perfect gas equation of state throughout), nevertheless Henry Norris Russell's several modified proposals remained highly influential throughout the late 1920s and early 1930s. The Russell proposal was widely discussed. An example is the Russell-evolution shown in the HR diagram by ten Bruggencate (1927, his Figure 30) or in the more accessible place in S04 (Chapter 17; Figure 17.1)

If the position of the subgiants in the HR diagram of A35 was correct as a sequence independent from that of the giants and dwarfs, the Russell proposal could not be correct. Figure 1 demonstrates the dilemma caused by the positioning of the Adams et al. subgiants relative to the giants. The mean magnitudes and spectral types of the giants and subgiants in Figure 1 are taken from the A35 summary diagram (their Figure 1). Clearly, either Russell's evolution proposal was wrong, or subgiants did not exist.

Concerning attempts to show that subgiants did not exist, consider a most curious paragraph in Adrian Blaauw's scientific autobiography written in 2004, long after the existence of subgiants had been established (Blaauw 2004). As a beginning astronomer at Leiden in the late 1930s, Adrian Blaauw had studied Gustaf Strömberg's papers and had concluded that "[the observational data on proper motions] could equally be represented without the subgiant branch."[2] This is an astounding conclusion in view of the increasing evidence from high weight trigonometric parallaxes and the accumulating evidence from spectroscopic parallaxes even at the time of Blaauw's graduate work (the 1930's). Later, in an extensive review of the calibration of luminosity criteria, Blaauw was unable to reconcile the A35 sequence with the still small sample of subgiants having reliable geometric distances (see §2.14 of Blaauw 1963, in particular his Fig. 5, which will be discussed in more detail below). Perhaps, Adrian Blaauw had not realized that the Mount Wilson subgiants of 1935 were linked with those of M67 in 1955, or with the *Hipparcos* trigonometric parallaxes of 1994, given that the A35 subgiants were two magnitudes brighter than, and not connected to, the main sequence. It is the purpose of this paper to show that the two groups of stars are identical by identifying the 90 Mount Wilson stars in a distinct sequence near $M_V = +2$ with *Hipparcos* subgiants.

2.2. Gamow's Conjecture

In a prescient letter from George Gamow to Walter Adams written in March 1944 and discovered by DeVorkin (2006) in the Adams papers of the Huntington Library archives, Gamow proposed a radically different scenario of evolution off the main sequence caused by hydrogen shell burning, shown in Figure 2 as track II. The subsequent expansion of the radius accommodates the subgiants and giants, and then a contraction (track III) gives the Wolf-Rayet stars, and thence to the white dwarfs. Gamow's diagram is remarkably close to the current evolutionary scenario. His conjecture was driven by the results of the model builders, of which he was the most tenacious. DeVorkin (2006) tells the story primarily from the many attempts at developing the theory in the early 1940s, all of which failed in important ways.

[2]See also very similar comments to this effect — but instead explicitly critiquing R.E. Wilson's work rather than Strömberg's — in the 1979 interview of Blaauw by David DeVorkin, available in the collection of oral histories on line by the American Institute of Physics (http://www.aip.org/history/ohilist/5002.html).

The breakthrough supporting Gamow's conjecture did come in the early 1950s, largely resulting from improved observational precision that clearly showed a subgiant sequence attached to the main sequence. Moreover, early evolution away from the main sequence was demonstrated in the Population I old Galactic clusters, M67 being the first in 1955. In these new data, the subgiants fit naturally into the observational picture. Gamow's conjecture had been essentially correct, but the breakthrough was most simply displayed before the eyes of the observers with their accurate, faint color magnitude diagrams that began to be produced en masse after 1952.

3. The 1957 Vatican Conference and Beyond

3.1. The Vatican Conference

Walter Baade's population concepts were discussed from many directions in an important conference in one of the first Semaine d'Etude sponsored and held at the Vatican in 1957 (O'Connell 1958). Among the many topics discussed were comparisons of the HR diagrams of Populations I and II relative to the color-magnitude diagram of M67.

To understand the discussion following a report by one of us on the color-magnitude diagram of stars within 20 parsecs of the Sun based on high weight trigonometric parallaxes, reproduced here in Figure 3 (Sandage 1958b, Figure 3, p. 295), we must understand the mindset at the conference concerning the age dating of the globular clusters, in particular the identification of the oldest Galactic clusters. A supposition, incorrect as it turned out, had been set by a report by one of us during the first days of the conference where a composite HR diagram of clusters of different ages, including M67, was compared with that of the old globular cluster M3 (Sandage 1958a, Figure 3, on p. 42), Here the main-sequence turnoff point for M3 is placed at nearly the same magnitude as that for M67.

Because globular clusters were acknowledged to be the oldest objects in the Galaxy, and because, by the aforementioned agreement of the M67 turnoff point with the M3 termination magnitude by incorrect alignments in the HR diagram, it was believed at the conference that the M67 subgiants would define the locus of the faintest field subgiants. But with the clear observational violation of that supposition by the faintest subgiants in Figure 3, especially seen by 31 Aql, μ Her, and δ Eri, something did not fit, hence the extended and lively discussion recorded in the conference report (O'Connell 1958, pp. 299-302).

The culprit was, of course, the detail of the placing of the turnoffs of M 67 and M 3 at the same magnitude in the aforesaid diagram. But it must be remembered that in 1957 the dependence of the main sequence on metallicity had not yet been discovered (Sandage & Eggen 1959), nor had the older galactic clusters NGC 188 and NGC 6791 been analyzed for their ages. The positioning of the main sequence according to metallicity has its own long history and is not especially germane to the subgiant story, but the discovery of clusters older than M 67 is relevant.

3.2. Many Field Subgiants Exist Fainter than those in M 67, NGC 188, and NGC 6791

Following the suggestions of Ivan King and Sidney van den Bergh, photometry of NGC 188 showed the cluster to have a turnoff luminosity fainter than M 67 (Sandage 1962). The placement of the M 67 and NGC 188 color magnitude diagrams as it was proposed in 1962 is given in Figure 4. This shows that the NGC 188 main-sequence turnoff is considerably fainter than that of M 67.[3]

Kinman (1965) showed that the galactic cluster NGC 6791 was even older than NGC 188. Many color magnitude diagrams have since been produced, perhaps the most accurate being that of Kaluzny & Rucinski (1995). Chaboyer et al. (1999) give a comprehensive review, which is brought up to date by SLV03. The importance of NGC 6791 is that it does define the lower envelope of the field subgiant distribution. There are many subgiant stars fainter than those M 67, but none statistically fainter than the subgiant sequence in NGC 6791, as demonstrated in Figure

[3] In Figure 4 note that the turnoffs of the three globular clusters are again placed at the NGC 188 turnoff magnitude. This is as incorrect as the placement of M 67 at the Vatican Conference. Hence, even as late as 1961 the position of the main sequence as a function of metallicity was not taken into account. A more correct diagram is in Sandage (1986, Figs. 5 and 6).

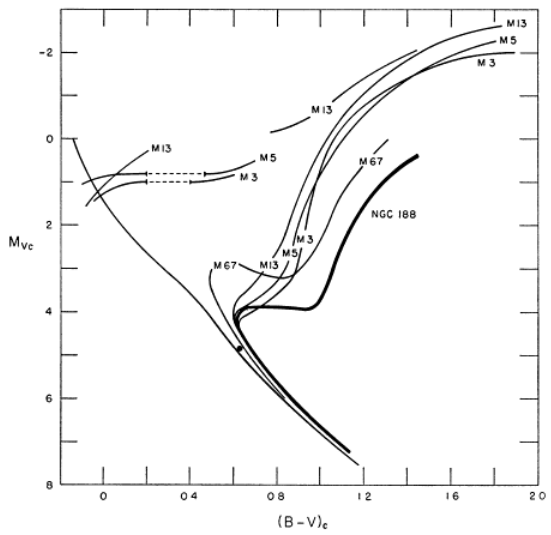

Fig. 4.— Solution to the problem of the Vatican Conference with the discovery of the older cluster NGC 188, whose subgiant sequence encompassed all known trigonometric field subgiants known at the time. Diagram from Sandage (1962, his Figure 10)).

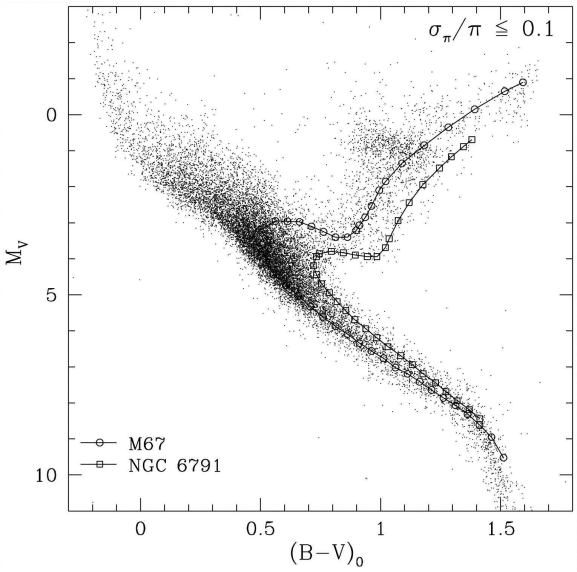

Fig. 5.— The HR diagram for *Hipparcos* field subgiants compared with those for the old galactic clusters M 67 (circles) and NGC 6791 (boxes). Many subgiants exist fainter than those in M 67 and NGC 188. NGC 6791 provides a good lower envelope for the population. Diagram from SLV03 (their Figure 12).

5 (adapted from Figure 12 of SLV03).

4. Comparing the Spectroscopic and Trigonometric Parallaxes

The purpose of the paper is to show that the ∼90 subgiants discovered by the Mount Wilson spectroscopists in the late 1920s and early 1930s, as calibrated from statistical parallaxes by Strömberg (1930), are truly subgiants according to *Hipparcos* trigonometric parallaxes. As an initial demonstration, we first compare the full A35 spectroscopic sample to the corresponding *Hipparcos* trigonometric database to highlight the general correlation between the two methodologies. Then, we will explore the key differences between the A35 and *Hipparcos* parallaxes and potential reasons for these differences. However, before proceeding with these analyses, we recount briefly the historical and physical premises that give foundation to the spectrocopic parallax method as employed by the Mt. Wilson astronomers.

4.1. The Mount Wilson Method of Spectroscopic Parallax

A comprehensive history of the Mount Wilson spectroscopic parallax program, work related to the project, and biographical sketches of the contributing scientists, is related in S04; the following is a synopsis of that account, but with some further explication of details relevant to the present story. The Mount Wilson sidereal spectroscopic program was one of the two "key" programs initiated on the 60″ Mount Wilson telescope upon its commissioning in 1908. The sidereal program hoped to target all stars with proper motions and was comprised of two parts: first, the measurement of radial velocities from prism spectroscopy with a slit to improve the wavelength resolution, and second, spectroscopic classification from these same spectra. With these data in hand, George Ellory Hale hoped that "real progress would be made for stellar evolution" (S04). The initial intent was to apply the then well-established Draper classification system, but the spectra, which spanned the range from λ4200 Å to λ4900 Å , were capable of reaching a resolution of 16 Å mm^{-1} (Adams & Kohlschütter 1914) and proved difficult to impossible to characterize following the established Harvard system, which had been devised

for spectra of a similar wavelength range but at a three times lower resolution. Even direct inspection of the plates by the Harvard team themselves failed to produce classifications consistent with those in the Draper catalog, which demonstrated that the Draper system of spectral classification was somewhat dependent on spectral resolution.

Thus, Walter Adams set out to "measure" spectral types from line ratios in lieu of "estimating" them from comparison spectra. First attempts were fruitful, but continued to produce offsets of order $\sim$2 classification bins, producing tension between the Mount Wilson and Harvard efforts. In attempting to resolve the tension, Arnold Kohlschütter first noticed that discrepancies in the line ratios were correlated with proper motion, which was a clear indication that a luminosity effect drove differences in the line ratios. This observation was the "seed" for the Adams & Kohlschütter (1914) work that demonstrated the necessity of special consideration for the well established dwarf and giant luminosity classes and, in turn, set the stage for the development of the technique of spectroscopic parallax. Soon after the 1914 publication, the attempt to "measure" stellar spectral classes directly from line ratios was abandoned (and a form of the Draper system adopted). Instead, realizing a spectroscopic distance technique was capable of building a large catalog of absolute magnitudes without limitations of geometric parallax, the Mount Wilson astronomers changed their focus to the spectroscopic parallax technique. This change of focus ultimately resulted in the A35 database of 4179 stars twenty years thereafter.

The initial luminosity criteria and an adaptation of the Harvard classification system to the higher resolution Mount Wilson spectra were published in a set of four papers presented to the National Academy of Sciences in 1916 that provided the full details of the techniques employed as of that date (Adams 1916a,b,c,d). The luminosity criteria were later expanded to both earlier and later stellar types, and such stars were incrementally added to the total A35 sample (most notably, Adams & Joy 1922; Adams et al. 1921, 1926). Since the publication of the A35 catalog the luminosity criteria for spectral classification have evolved, but many of these early line ratios remain fundamental to luminosity classification (see discussions by Gray & Corbally 2009, and references therein).

It was noted in Adams et al. (1921) that spectral types F through G exhibited a "continuous change of absolute magnitude with line intensity", which contrasted with the "marked discontinuity" in the resulting magnitude distribution for the K and M types, which separate into distinct giant and dwarf classes within the solar neighborhood. Strömberg (1930, 1932) later isolated the subgiant luminosity class as the entity that connected the well known dwarf and giant sequences for the F and G spectral types using absolute magnitudes derived from statistical parallax. Not all of the spectral lines associated with these classes exhibited a strong continuum of line strengths; the most important for the subgiants were λ4077Å, λ4215Å, λ4324Å, and λ4454Å. The lines λ4077Å and λ4215Å from Sr II were identified as being sensitive to surface gravity as early as Adams (1916b).[4] The line λ4454Å from Ca I is only used for types F8 to G in the detailed classification notes given by Adams et al. (1921). The Cr I line λ4324Å is not discussed specifically until A35 (see their Table 1). The well-established empirical sensitivities to surface gravity for the majority of the luminosity sensitive lines were given a physical underpinning by Saha (1921), who vividly illustrated the effect of electron number density in populating the ionized metal states. As atomic theory progressed, a series of papers led by Walter Adams connected the parallel revelations produced via empirical study of stellar atmospheres and those by pure theory (Adams & Russell 1928; Adams 1929, 1933), and, in particular, highlighted the ability of observational astronomers to infer the physical conditions of stars long before there was a theoretical framework. Most notable is the work of Adams & Russell (1928), which combined the physical measurements of stars from binary observations by Russell (1914) with the Mount Wilson line-ratio technique to conclude that it was feasible to determine the physical conditions of stellar atmospheres from appropriately chosen line ratios, more specifically those line ratios conforming best

[4] Adams note that these lines were "brighter in the spark than in the arc" with respect to spectra obtained of the solar limb and upper chromosphere compared to the solar surface.

to the theoretical predictions of line strengths from the Saha equation and were, effectively, unaffected by physics yet to be fully discovered.

While the electron-density dependence of the Saha ionization equation is, indeed, the underpinning theory for why ionized metal lines are enhanced in stars of lower surface gravity, this was not the only physics affecting the four lines used for exploration of the subgiants. In fact, two of the four lines used by A35 have additional properties that make them even more sensitive to subtle changes in surface gravity — the Sr II lines at λ4077Å and λ4215Å are resonant lines that arise from the ground state of the atom. Many of the other line ratios utilized by A35 (see their Table 1) are meta-stable levels of Fe II and Ti II, whose lower states are forbidden by quantum selection rules. The reason for the particular sensitivity of λ4324Å of Cr I and λ4454Å of Ca I to surface gravity and, in consequence, their utility for the early identification of subgiants is due to enhanced collisional broadening with in the atmospheres of dwarf type stars. Modern spectral classification takes these, and other, detailed effects into consideration.[5]

Modern spectral classification can also exploit extremely high resolution spectroscopy, which, when compared to synthetically generated spectra, permits an even more nuanced portrait of stellar atmospheres. In particular, this body of work has made more apparent the underlying flaw of the spectroscopic parallax approach: it remains unclear whether, given the numerous variables that affect stellar luminosity all stars of a given spectral class and luminosity type *do* have the same absolute magnitude (in particular, the effect of microturbulence is still an area of active exploration, e.g., Jaschek & Gomez 1998). Stated differently, the true intrinsic dispersion of a given stellar class and luminosity type remains poorly constrained. To evaluate such a quantity, one requires sufficiently many stars with high weight trigonometric parallaxes to fully populate a sample for each spectral class and luminosity type — something that is not fully feasible for even the *Hipparcos* sample (see discussion in Jaschek & Gomez 1998), given the need for obtaining complementary moderate resolution spectroscopy and hiqh quality photometry for a large number of stars in each classification bin. A full understanding may be first be feasible with the combined astrometric, photometric and spectroscopic datasets provided by *GAIA* in the near future (more than a century after the start of the Mount Wilson spectroscopic program). In the end, the notion of "measured" luminosity classes following the Mount Wilson criteria was abandoned by the astronomical community for the reasons already presciently argued by Morgan (1937) that "unreconcile-able difficulties of nomenclature" would occur with such a measured system, whose reduction curves would be highly sensitive to the specifics of the spectral data and analysis techniques employed for a given study. While the concept of "measured spectral typing" was ultimately abandoned, it is the subject of this work to evaluate whether the distances inferred via the spectrscopic parallax technique where in themselves useful for advancing the understanding of stellar evolution with respect to the aforementioned problems with "aging" stellar sequences.

4.2. The A35 Subgiants in the Context of the H-R Diagram

To test whether the Mount Wilson-identified subgiants are real, we employ the trigonometric parallax and photometric magnitude data contained in the revised *Hipparcos* catalog (Perryman et al. 1995; van Leeuwen 2007a,b, 2008). Matches between the entire Mount Wilson list of 4179 stars as compiled by A35 to the *Hipparcos* catalog were made solely through the star names — predominantly the Henry Draper number, available for 90% of the stars — as identified in the A35 catalog.[6] We present the full matched catalog in the HR diagrams of Figure 6. We note that the A35

[5] For more information, we refer the interested reader to the textbook on the subject by Gray & Corbally (2009).

[6] Because an electronic version of the extensive Mount Wilson data table, spanning some 93 pages of the Astrophysical Journal, does not exist, these pages were scanned into digital form and then passed through optical character recognition software (OCR) to compile output tables. The OCR software required considerable training because the font-face and typesetting styles used in the 1935 print journal are not included in standard OCR templates. The output digital tables were then reformatted and checked manually for errors. Detailed data for only the subgiants are presented directly in this paper, but a digital version of the full A35 database will be made available online.

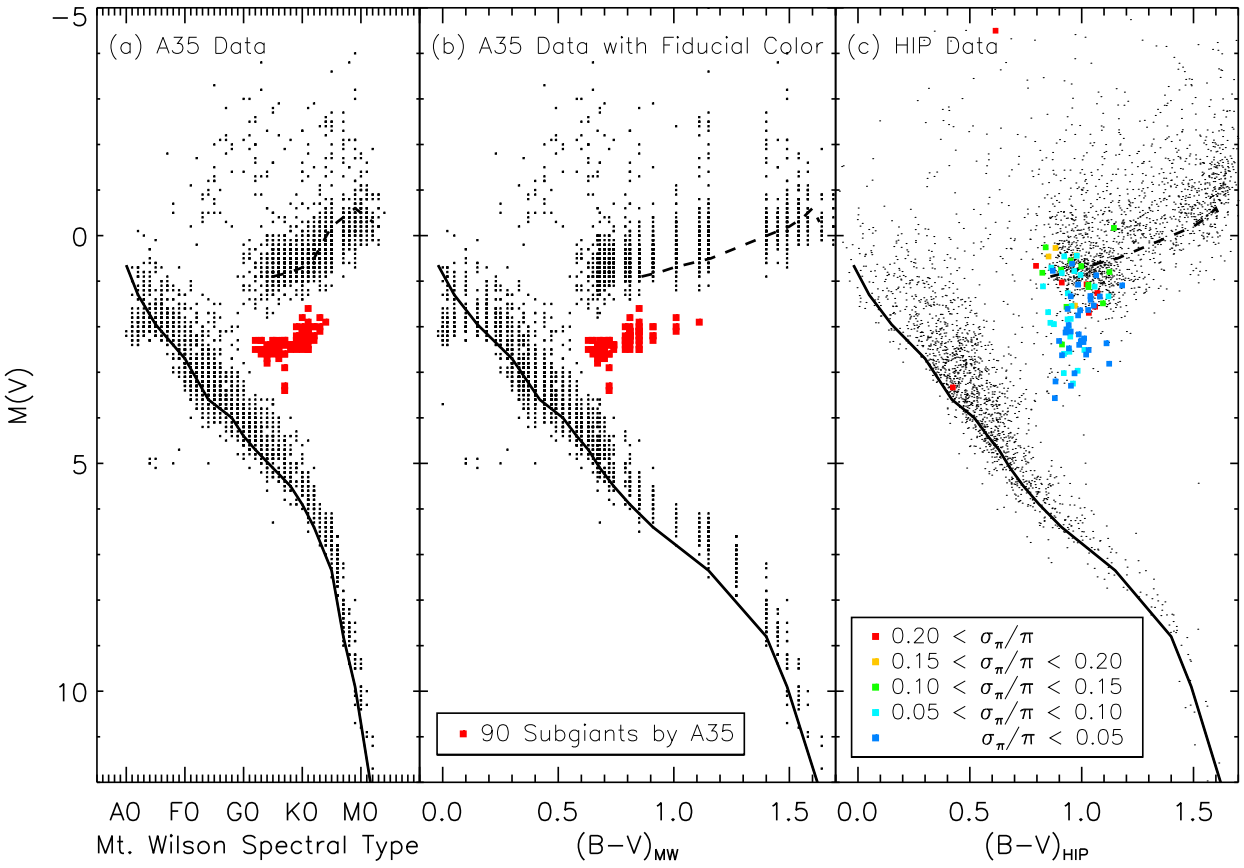

Fig. 6.— The HR diagram for the 90 Mount Wilson subgiants from A35 in panel (a) plotted by spectral type and in panel (b) by conversion to a fiducial color, compared to (c) the van Leeuwen (2007a,b, 2008) *Hipparcos* data for the same stars from the listings in our Table 1. The solid line is an example main sequence and the dashed line is an example red giant sequence, with absolute magnitudes taken from Johnson (1966) and colors from Schmidt-Kaler (1982). Red filled squares in panels (a) and (b) indicate those stars we take as those identified as subgiants by A35. In panel (c) these same stars are color coded by their fractional parallax error (σ_π/π). This figure demonstrates that the bulk of the 90 stars identified in A35 are in fact subgiants.

catalog contains spectral types, apparent magnitudes, absolute magnitudes and the derived spectroscopic parallax, whereas the *Hipparcos* catalog contains apparent magnitudes and trigonometric parallaxes. It is also important to bear in mind that the colors and apparent magnitudes in the *Hipparcos* catalog come from a diverse set of ground-based sources, but we find the data to be reliable and homogeneous enough to make our point (i.e., even with whatever systematic and random uncertainties may lie within the catalog, the correlations we find are strong). In Figure 6a we reproduce the HR diagram from the original A35 paper (their Figure 1) based on our digitalization of their original catalogue while in Figure 6b we convert the A35 spectral type to a fiducial $B-V$ color using the standard observed values defining each spectral class as presented in Schmidt-Kaler (1982). In Figure 6c, we convert the *Hipparcos* trigonometric parallaxes to absolute magnitudes using the apparent magnitude information provided in that catalog.

The stars considered to be subgiants are not explicitly identified in A35. Instead, the authors refer to "stars of type G and K somewhat fainter than normal giants" and a mean magnitude of $M_V \sim 2$. We used the A35 description to identify their subgiants as those stars having $1.6 < M_V < 3.4$ and spectral types from G2 to K4 in the A35 tables; these stars are highlighted as red filled boxes in Figures 6a and 6b. Fortunately, the majority of the stars we take to be the A35 subgiants are clearly separated from the red giant and main sequences in Figure 6a, consistent with the A35 description, and there are few ambiguous examples. We identify 90 such stars as likely to be the A35 "subgiants", and this matches well their statement that they see "about 90 some stars" meeting their criteria.

In Figure 6c these same stars are highlighted and color-coded by their *Hipparcos* fractional parallax error, $\sigma(\pi)/\pi$, which is a standard measure of the reliability of trigonometric parallaxes. The majority of the stars highlighted in Figures 6a and 6b remain "subgiant-like" in the *Hipparcos* HR diagram of Figure 6c, but the clean separation between the subgiants, giants and main sequence in the A35 data is no longer present; instead they form the more familiar continuous evolutionary sequence from the main sequence to the red giant branch. We emphasize that no Lutz & Kelker (1973) corrections have been applied to the *Hipparcos* data, but that such corrections are on a scale that will not affect the overall impression given in Figure 6c. We discuss the potential effects of the Lutz-Kelker bias in more detail in Section 4.4.

Table 1 presents the relevant A35 and *Hipparcos* data for the 90 stars identified as subgiants in Figure 6 (the red boxes). Most of the columns of Table 1 are self explanatory. Column 9 supplies the value of $\sigma(\pi)/\pi$ from *Hipparcos*, a useful parameter guiding the interpretation of results. The crucial columns are 10 and 11 where the Mount Wilson absolute magnitudes determined from the spectra are compared with the *Hipparcos* trigonometric values. Absolute magnitudes from the *Hipparcos* data are derived by combining the trigonometric parallaxes and apparent magnitudes, while the values adopted by the Mount Wilson astronomers are given directly in the catalogue of A35.[7]

Despite the remarkable correspondence between the spectroscopic and trigonometric absolute magnitudes in Table 1, there are two pronounced differences. First, unlike what is seen in the modern *Hipparcos* panel (Figure 6c), the subgiant sequence as positioned by Adams et al. (Figures 6a and 6b) was neither attached to the main sequence on the left or onto what in later HR diagrams was the base of the first ascent giant branch on the right. Second, the overall scatter along each sequence in the A35 diagram (Figures 6a and 6b) is smaller than — or at least on par with — that of the more accurate, modern magnitudes in the corresponding *Hipparcos* diagram (Figure 6c). This second effect is most dramatic for the subgiant sequence in A35 (colored points in Figure 6), which is nearly horizontal and spans only ~ 1 magnitude of M_V.

Given these morphological differences in the subgiant branch, the significance of the subgiants for stellar evolution were not realized at that time. If it had been, however, the placement of these stars could not be explained by the prevailing

[7] In particular, A35 states that their subgiant stars were "selected based on the strength of the lines 4077, 4215, 4324 and 4454. Special reduction curves based on trigonometric parallax were used to determine the absolute magnitudes of these stars."

Russell giant-to-dwarf stellar contraction scenario (Figure 1). In contrast, subgiants are a natural phenomenon for the evolutionary model proposed with Gamow's conjecture (Figure 2). More specifically, the position of the subgiants in Figure 6 is easily explained as stars transitioning from the main sequence to the first-ascent giant branch after hydrogen core exhaustion. As summarized above, this understanding of the role of subgiants in stellar evolution, in particular as relative age indicators for single stellar populations, was not to be fully conceptualized until the early 1950s.

Nevertheless, even if it was not fully appreciated or accepted at the time, the Mount Wilson spectroscopists had, in fact, discovered the subgiant sequence from their spectral line classification method. Meanwhile, from independent considerations, Gamow had proposed the correct evolution scenario, but it was a decade before his unpublished conjecture was substantiated based on observations of the main-sequence turnoffs and subgiant branches in a number of galactic and globular clusters in the 1950s and 1960s.

4.3. Magnitude Comparisons

Although the visual comparison of the Mount Wilson HR diagram and CMD (Figures 6a and 6b, respectively) with the corresponding *Hipparcos* CMD (Figure 6) is quite illustrative, we directly compare the two sets of absolute magnitudes for all stars in the Mount Wilson tables in Figure 7. Remarkably, a strong correlation is found among all luminosity classes and spectral types. These results convey the striking efficacy of the Mount Wilson spectroscopists to get the true absolute magnitudes from spectra, and, in particular, for the previously unidentified subgiant class (those stars with $1.6 < M_V < 3.4$ and spectral type from G2 to K4).

There are, however, some differences visible in Figure 7 and these differences vary with luminosity class. The main-sequence stars by far exhibit the cleanest correlation, $\langle M_{V,\mathrm{MtW}} - M_{V,Hipparcos} \rangle = 0.18 \pm 0.02$; this is largely because the A35 absolute magnitudes of these stars were calibrated using the trigonometric parallaxes available to the Mount Wilson astronomers at that time.

The subgiant and giant branches, on the other hand, exhibit a correlation that is visibly shallower than that for the main sequence. Additionally, the mean offsets for the giants and subgiants are substantially larger: for the giants $\langle M_{V,\mathrm{MtW}} - M_{V,Hipparcos} \rangle = 0.46 \pm 0.02$ and for the subgiants $\langle M_{V,\mathrm{MtW}} - M_{V,Hipparcos} \rangle = -0.24 \pm 0.07$. From visual inspection of Figure 7, however, it is clear that those stars with the lowest σ_π/π agree better with the A35 results (cyan and blue in Figure 7). If we restrict to $\sigma_\pi/\pi \leq 0.05$, then we have, for the main sequence, $\langle M_{V,\mathrm{MtW}} - M_{V,Hipparcos} \rangle = 0.06 \pm 0.02$, the giants, $\langle M_{V,\mathrm{MtW}} - M_{V,Hipparcos} \rangle = 0.15 \pm 0.04$, and the subgiants, $\langle M_{V,\mathrm{MtW}} - M_{V,Hipparcos} \rangle = -0.12 \pm 0.02$. These comparisons are summarized in Table 2.2. Unlike those of the main-sequence stars, the absolute magnitudes of the evolved stars were calibrated against a sample of *statistical* parallaxes, which may explain the differences in the behavior of the evolved versus main sequence stars in Figure 7.

Although the overall similarities between the A35 and *Hipparcos* absolute magnitudes are strong, the magnitude differences are not insubstantial. Furthermore, that the severity of the magnitude differences are correlated with luminosity class may help to explain why the A35 subgiant sequence was not appreciated in the literature of the time. To explore these differences, we first consider the potential effects of the Lutz-Kelker Effect in the *Hipparcos* absolute magnitudes in Section 4.4 as a potential source of the observed mean magnitude offsets in Figure 7. In Section 5, we revisit the historical discussions of the A35 absolute magnitudes to reassess published criticisms of the A35 calibration technique.

4.4. The Lutz-Kelker Effect

The Lutz-Kelker Effect (LKE, hereafter) is an insidious and complex bias afflicting trigonometric parallax samples that was discussed in detail by Trumpler & Weaver (1953) and then parametrically formalized by Lutz & Kelker (1973). The effect is defined as an offset between the mean absolute magnitudes for classes of stars as determined from trigonometric parallax samples and the true mean absolute magnitude for that stellar class. Because the effect is only identified in the mean values derived for a stellar class its effect on individual stars is difficult to intuit. Here

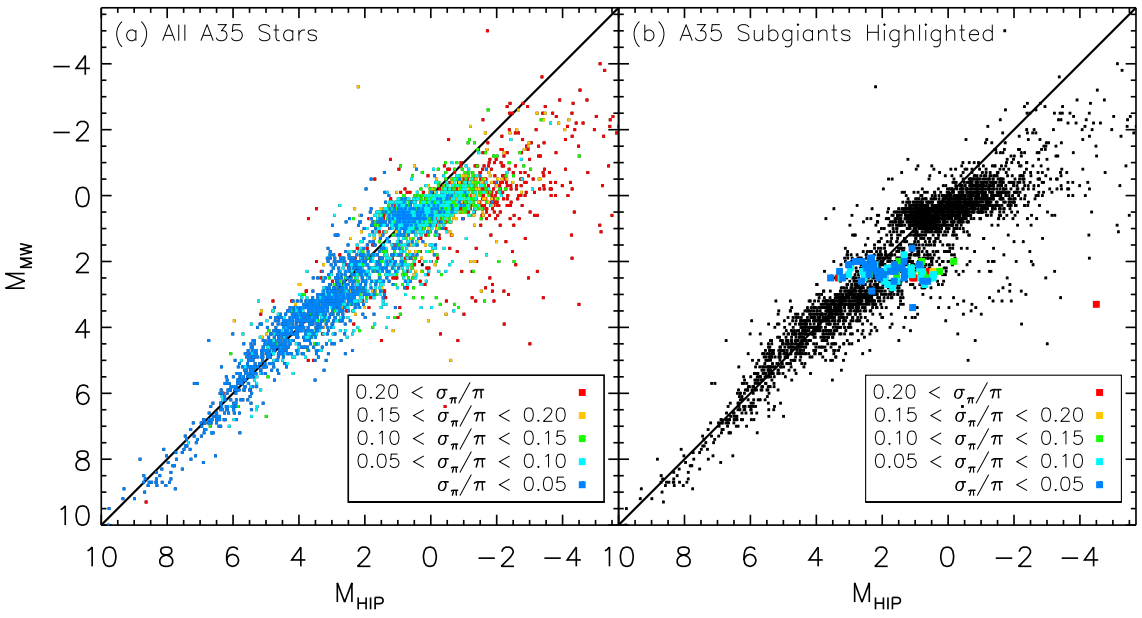

Fig. 7.— Comparison of Mount Wilson spectroscopic absolute magnitudes — in panel (a) for the full A35 sample and in panel (b) highlighting the 90 subgiants — with *Hipparcos* absolute magnitudes for the same stars. The color coding in both panels is by the fractional trigonometric parallax error, or σ_π/π. The A35 subgiant absolute magnitudes are incredibly compressed (spanning only ~ 1 magnitude) compared to those of *Hipparcos* (spanning ~ 4 magnitudes), both of which are given in Table 1.

we first review the origin of the bias, and use a brief schematic analysis to assess the severity of the LKE in the matched A35-*Hipparcos* sample. A more rigorous derivation of the relevant LKE parameters is given in Appendix A.

At the parallax limit of a sample, the volume element just outside of the limit is larger than the one just inside. A symmetric error distribution applied to both volume elements will systematically scatter more stars into a sample than out — because the outer (and larger) volume element is likely to have more stars (though the magnitude of the effect clearly depends on the underlying stellar distribution). This asymmetrical scattering has the consequence that, statistically, more stars of a given stellar class will be scattered into a parallax-limited sample than out. The parallax for a star scattered into the sample is obviously observed to be larger than the true value, and by consequence, both the inferred distance and intrinsic flux are underestimated. Thus, the mean absolute magnitude of a particular stellar class within the sample will be offset compared to the true intrinsic mean magnitude for that class; this offset is defined as the Lutz-Kelker correction.

Early numerical explorations of the bias parameterized it by $\sigma(\pi)/\pi$, the ratio of the error in the parallax to the parallax itself (Lutz & Kelker 1973). The bias is found to be significantly pronounced when $\sigma(\pi)/\pi \gtrsim 0.2$. Because the parallax error is nominally set by the systematics of the trigonometric parallax program (e.g., temporal baseline, detector pixel scale, overall flux sensitivity), the LKE grows in its relevance towards the volume limit of the survey. Though the LKE is defined as a statistical offset for a *sample* of stars of a given class, Lutz & Kelker (1973) argue that their defined correction could be used to correct the derived absolute magnitudes for *individual* stars, and it often has. More recently, the logic behind this practice and Lutz & Kelker's original suggestion that the correction could be applied to individual stars has been challenged (van Leeuwen 2007a; Smith 2003; Francis 2014). Regardless of this "Lutz-Kelker Paradox", it is nonetheless naturally the case that stars with a larger parallax error will show a larger error in derived absolute magnitudes, and, as a class, would be expected to exhibit a larger systematic offset; it is our goal to assess whether this phenomenon has any significant effect in our comparison of A35 absolute magnitudes to those derived from *Hipparcos* parallaxes. In Figure 7a, individual stars are color coded by σ_π/σ. As anticipated, those stars with higher fractional trigonometric parallax errors, show, on average, the largest deviations from the A35 magnitudes — though the degree of this scatter is highly dependent on the luminosity class.

Is the LKE primarily responsible for the magnitude offsets between A35 and *Hipparcos* (Section 4.2; Table 2)? The LKE as applied to the *Hipparcos* catalog, has been explored by numerous authors, including, but not limited to, Oudmaijer et al. (1998), Brown et al. (1998), and van Leeuwen (2007a). Generally, it is advised to reject all stars with fractional errors greater than 10% or $\sigma(\pi)/\pi > 0.10$, but a full treatment of the LKE, and any other relevant biases, requires detailed modeling of the specific sample in question (e.g., Sandage & Saha 2002; van Leeuwen 2007a; Smith 2003; Francis 2014). While the very form and magnitude of the LKE has also been reassessed and debated (see previous references) we adopt the formalism of Sandage & Saha (2002) for our calculations, which are primarily illustrative; because subsequent treatments of LKE tend to find bias corrections of an overall smaller magnitude than those of Sandage & Saha (2002), our examples can then be seen as an upper limit to the expected LKE influence on the *Hipparcos* data.

To place the magnitude offsets between the Mount Wilson and *Hipparcos* data in context, we consider the magnitude and distance distribution for the A35 stars, for which the faintest is $V = 10.5$, the majority are brighter than $V = 8$, and the most distant is only $d = 500$ pc. In comparison, *Hipparcos*, is complete for $m_V = 7.3$ to 9.0, reaches a limiting magnitude of $m_V = 12.4$, and has a median parallax precision of 0.97 mas (i.e., that of a 1000 pc star). As given in Table 2.2, the magnitude differences between A35 and *Hipparcos* data are generally small compared to the precision feasible for the A35 magnitude measurements, especially so when restricted to $\sigma(\pi)/\pi < 0.05$. Using the $\sigma(\pi)/\pi < 0.05$ criterion, a star with the median parallax error would have a corresponding distance ($d = 50$ pc) well within the *Hipparcos* sampling volume, and at a magnitude for which the *Hipparcos* sample is complete. Using this fiducial, we conclude that any trigonometric

parallax bias offsets in our sample are going to be quite small, and unlikely to influence strongly the impression of the magnitude comparisons given in Section 4.2.

This rough assessment of the role of the LKE in our comparison suggests that the LKE does not significantly influence the general impression given in Figures 6 and 7. In Appendix A, a detailed numerical exploration of the LKE along the lines of Sandage & Saha (2002) supports the conclusion that LKE is not significantly affecting the *Hipparcos* data for the A35 sample.

5. Reconciling Criticisms of the A35 Subgiant Sequence

In the previous section we showed that the subgiants discovered in the A35 dataset are bona fide subgiants in the *Hipparcos* catalog. In our historical account of the discovery of subgiants, we have discussed in detail why the prevailing stellar evolution theory in 1935, the Russell contraction scenario, may have biased the immediate interpretation of the A35 results at the time of publication. We have not, however, discussed the reasons why the A35 data, which show a clear subgiant sequence, were insufficient to challenge Russell's hypothesis (Figure 1).

Numerous works investigated the reliability of the A35 database, as it remained one of the largest catalogs of absolute magnitudes well into the middle of the 20th-century. A full discussion of this body of work, as well as rigorous comparisons to pre-*Hipparcos* databases, is given by Blaauw (1963). Our goal, to show conclusively that the Mount Wilson spectroscopists discovered subgiants in their seminal 1935 work, requires addressing the concerns expressed for the A35 calibration methodology by revisiting the doubts on its reliability. More specifically, we must determine whether specific, cited problems artificially created the subgiant sequence in Figure 6.

First, we briefly reiterate the methods employed by A35: Adams & Kohlschütter (1914) first detected a correlation between specific sets of line intensities and the proper motion of the star — more specifically, that for a given spectral type the line intensities for small and large proper motion stars were systematically different. From this initial discovery, a series of line ratios were established as a means of identifying both the spectral type and the absolute magnitude (luminosity) of a star from spectroscopy. This work became the basis for the two decade observing campaign that culminated in the 4179 member catalog in A35.

This method of "spectroscopic parallax" itself was never a point of contention in the literature; rather, it was the calibration of the technique against existing parallaxes that raised concerns. The calibration required two key decisions: (i) a choice of a suitable external calibration sample, and (ii) the grouping of the existing spectral line data into appropriate classes. For the former, Gustaf Strömberg's parallax program was selected by A35 as an ideal calibration sample, even though his statistical parallax sample for giant stars suffered effects from Malmquist bias. Clearly, this bias would propagate into the A35 catalog, but in manner difficult to intuit; concerns over this problem led to a general distrust of the reliability of the absolute magnitudes for giant stars, and a dismissal of the A35 subgiant sequence as likely attributable to the effect. For decision (ii), the Mount Wilson spectroscopists assumed that the observational scatter was driving the distributions (and not intrinsic differences between stars) and thus chose to group the line ratios based on the peaks in their distribution — a process that can suppress outliers (see Appendix B) — instead of using an independent criterion to classify the stars by spectral type and luminosity class that would yield a more representative scatter. The effect of this choice on the A35 catalog is less immediately obvious, but, as will be explained in Section 5.2, it resulted in an overall suppression of the true observational errors in the A35 sample. This suppression is visible in Figures 6a and 6b as the narrow vertical dispersion across all sequences (main, subgiant, and giant), but most conspicuous for evolved star sequences in Figure 6, and the overall "disconnected" nature of all three luminosity sequences in the HR diagram.

Both of the above choices in the calibration process by the Mount Wilson spectroscopists were heavily discussed in the literature, and became a source of contention regarding the legitimacy of spectroscopic parallaxes for any stars not on the main sequence, i.e., any stars not calibrated directly to trigonometric parallaxes. Adrian Blaauw in his 1963 review of luminosity criteria com-

ments that the complex statistical arguments over the A35 calibration in the literature "may have created the impression that these systematic errors are of an intricate nature and the Mount Wilson results therefore less useful [than other absolute magnitude samples]" (Blaauw 1963). With more geometric parallaxes in hand, Blaauw demonstrated the efficacy of the A35 data for the dwarfs and we repeat this analysis with *Hipparcos* parallaxes to demonstrate the same for the giants and the subgiants. We first address the cited concerns over the effects of Malmquist bias in the selected calibration sample on the A35 survey in Section 5.1. Then we qualitatively describe the problems with the A35-adopted calibration methods in Section 5.2 and correct the A35 magnitudes for these effects in Section 5.2.2. A detailed quantitative derivation parallel to the more qualitative discussion in Section 5.2 is given in Appendix B.

5.1. A Test for an Incompleteness (Malmquist) Bias in the 1930 Calibration by Strömberg

The A35 sample featured three luminosity classes cleanly distinguished by their position in the HR diagram: dwarfs, subgiants and giants. The absolute magnitudes were determined from spectral line ratios using independent calibrations for each luminosity class and spectral type. More specifically, the main-sequence stars were calibrated with absolute magnitudes from trigonometric parallaxes, whereas the, on average, more distant subgiants and giants were calibrated to statistical parallaxes. In Figure 7, the difference in calibration techniques is obvious, with the Mount Wilson absolute magnitudes calibrated to the statistical parallaxes showing a stronger deviation from the *Hipparcos* values than those calibrated to trigonometric parallaxes.

The statistical parallaxes used to calibrate the giant and subgiant sequences were derived using a sample complete to an apparent magnitude of $V = 5.9$ (Strömberg 1930), whereas the full A35 sample contains significantly fainter stars ($V = 10.5$). In a sample that is not volume limited, intrinsically luminous objects are systematically over represented because they can be surveyed over a larger volume of space than intrinsically fainter objects at the same apparent magnitude limit. The Strömberg (1930, 1932) calibration sample was subject to this "Malmquist bias", which skews the mean absolute magnitude of a sample systematically brighter than the true mean absolute magnitude. Thus, with their samples calibrated with the Strömberg data, the A35 absolute magnitudes calculated for the subgiants and giants sample would be systematically brighter than those that would be calibrated against an unbiased sample.

The bias would also apply to any dwarf stars misidentified as giants and for which the giant star calibration were utilized. Under one interpretation, the A35 subgiants could be stars misplaced in the HR diagram and made systematically even brighter due to the Malmquist bias. Meanwhile, with the Malmquist bias in the giant star calibration skewing the magnitudes of real giant stars systematically brighter, the separation between luminosity classes would be exaggerated as well, and presumably contribute to the disjoint appearance of the subgiants in the A35 HR diagram.

To judge the viability of these concerns, we can diagnose the role of the Malmquist bias, and even treat its effects, on the A35 magnitudes. The Spaenhauer diagram (see review on the topic by Sandage 2001), an effective tool for detecting and correcting the effects of the Malmquist bias, plots the absolute magnitude (M) versus the distance to the object (D). In the Spaenhauer diagram, the presence of the Malmquist bias produces fictitious behavior in the magnitudes with respect to distance. A key requirement for diagnosing the Malmquist bias in a sample is having distance estimates that are independent of the luminosity estimates being explored. One means to diagnose and assess the strength of the Malmquist bias is to assess how the implied behavior of data in the Spaenhauer diagram changes as fainter samples are added incrementally (Sandage 2001).

We demonstrate this technique in Figure 8, where we plot (panel a) the *Hipparcos* absolute magnitudes versus the trigonometric distance, which at the maximum radius in this sample, $D < 400$ pc, should not show any significant effects due to this bias. The thick black dashed line represents the flux limit of the Strömberg statistical parallax sample ($V = 5.9$). For the stars with $m_V < 5.9$ ("x" symbols) in Figure 8a, those at the greatest distance (the giants) tend to have an intrinsically brighter absolute magnitude. Were one limited to only a $V < 5.9$ sample, one would *incorrectly* infer that there are no intrinsically

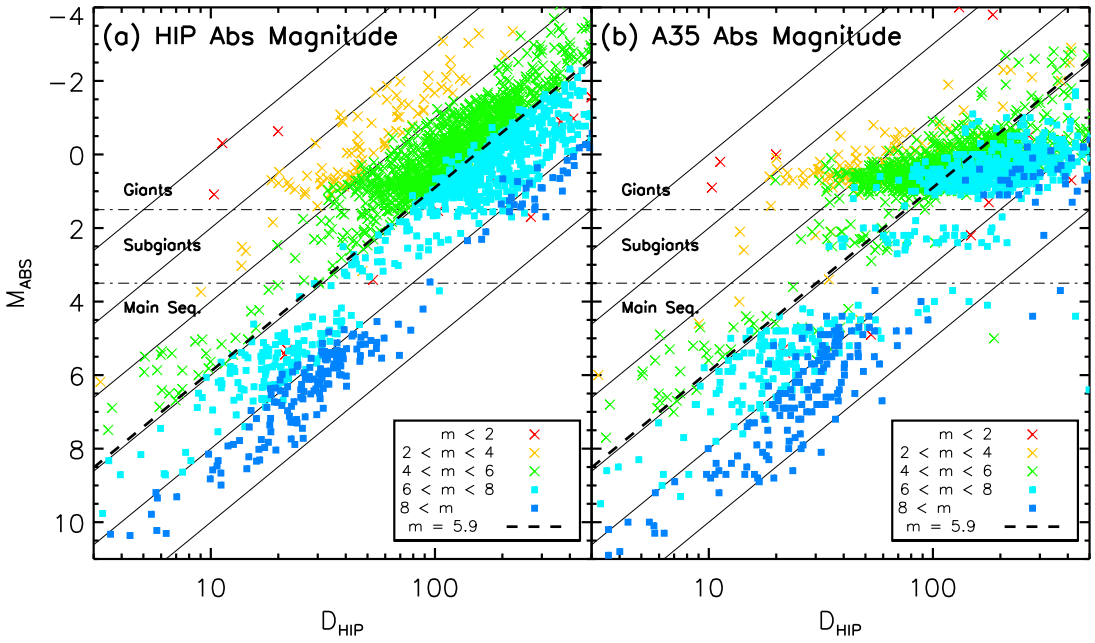

Fig. 8.— Spaenhauer diagrams for the matched (a) *Hipparcos* and (b) A35 magnitude samples, both of which plotted using the *Hipparcos* distances (D_{HIP}). The thin black lines are the apparent magnitude limits of 0, 2, 4, 6, 8 and 10 magnitudes. The horizontal dot-dash lines mark the separation between luminosity classes of dwarf, subgiant, and giant, while the dashed line separates stars brighter (crosses) and fainter (squares) than $V = 5.9$. The Malmquist bias has the effect of creating intrinsic luminosity trends with distance appear at the faint limit of a sample. As apparently fainter stars are added any trends imposed by the Malmquist bias will disappear, whereas real trends will persist with the fainter samples. Panel (b) shows that the subgiants persist as a distinct group beyond $V = 5.9$.

faint stars beyond 40 pc. But when stars having fainter apparent magnitudes are added (the filled boxes), the previously apparent behavior — i.e., that there are no intrinsically faint stars beyond 40 pc — disappears at those distances at which the sample is now complete. While this particular demonstration is quite simple, in other datasets exploring more complex astronomical questions the Malmquist bias can induce many false impressions (see a historical review by Sandage 2001).

Figure 8b is similar to Figure 8a except the Spaenhauer analysis is applied to A35 absolute magnitudes, which are also plotted against the *Hipparcos* distance (M_{HIP}). In Figure 8b we see the same behavior as in Figure 8a for the main-sequence stars ($M > 3.5$); again, the magnitude trend with distance disappears as fainter apparent magnitude samples are considered. If we restrict ourselves to those stars with $V > 5.9$, the giants and subgiants are nearly horizontal in magnitude with respect to distance and the two branches are offset from one another. While both trends — the horizontal shape and the separation between branches — are shown to be specious by comparison to the pure *Hipparcos* data in Figure 8a, we can also see by Figure 8b that the specious character is not introduced by the Malmquist bias but that, in fact, these features are intrinsic to the A35 absolute magnitudes: As we view increasingly fainter samples in Figure 8b, the shape of the giant and subgiant branches and their separation do not change. This demonstration effectively dispels the notion that the A35 sample for giants and subgiants was significantly compromised by the Malmquist bias in the calibration of Strömberg (1930), and that this bias does not readily account for a false introduction of the subgiant sequence nor does it fully account for the shape of the giant branch. For a full exploration of these criticisms and their implications in the literature of that time, we refer the reader to Blaauw (1963), in which the Malmquist bias could not be fully tested owing to the still relatively small number of luminous stars with trigonometric parallaxes.

5.2. Correcting the A35 Calibration Method

Having determined that the Malmquist bias is not the source of the morphological differences between the A35 and *Hipparcos* CMD, we now explore the A35 calibration as the culprit. For the A35 data, visual estimates of relative spectral line intensities were calibrated empirically to absolute magnitudes derived from trigonometric parallaxes for the dwarfs and to statistical parallaxes for the evolved stars (Strömberg 1930). In this section, we qualitatively describe the luminosity calibration used by A35 and explore how their process induced systematic errors in their derived absolute magnitudes. A complementary quantitative derivation of these errors is given in Appendix B.

Combinations of line intensities had already been shown to classify the stars by their spectral type and in Adams & Kohlschütter (1914), the Mount Wilson spectroscopists discovered a set of line intensities that were sensitive to luminosity. Once the Strömberg (1930) sample of 1647 stars became available, the Mount Wilson spectroscopists began to explore how to exploit it for calibrating their data. The (Strömberg 1930) stars were first grouped into their spectral classes based on the Mount Wilson criteria. Within each of these classes, the line intensities were observed to cluster around certain mean values (I_o), and these were correlated with the proper motion of the star (a proxy for the distance to the star). Each of these distinct line intensity groups represented one of the classes from the modern luminosity classification system, though at the time this was primarily limited to the dwarf and giant classes. However, from his calibration sample of 1930, Strömberg had already noted the existence of stars intermediate in luminosity between the giants and dwarfs and he termed these stars "subgiants" for their location relative to the giant branch. Thus, for each of the *three* groups of line intensity, a calibration curve was determined as a linear regression of the form $M = \alpha I + \beta$ (example curves are given in Adams 1916a, their Fig. 1). These calibrations, ultimately derived from the Strömberg sample of 1647 stars, were then applied to the full Mount Wilson sample of 4179 stars in the seminal 1935 catalog.

Though at a cursory glance this calibration procedure seems valid, there is a key flaw in the method: the line intensities were used *both* to determine calibration groupings *and* to derive the calibration curves. Because these two separate steps rely on the same underlying data, they are not independent (impartial). The calibration is, therefore, "partial" to those line intensities tightly

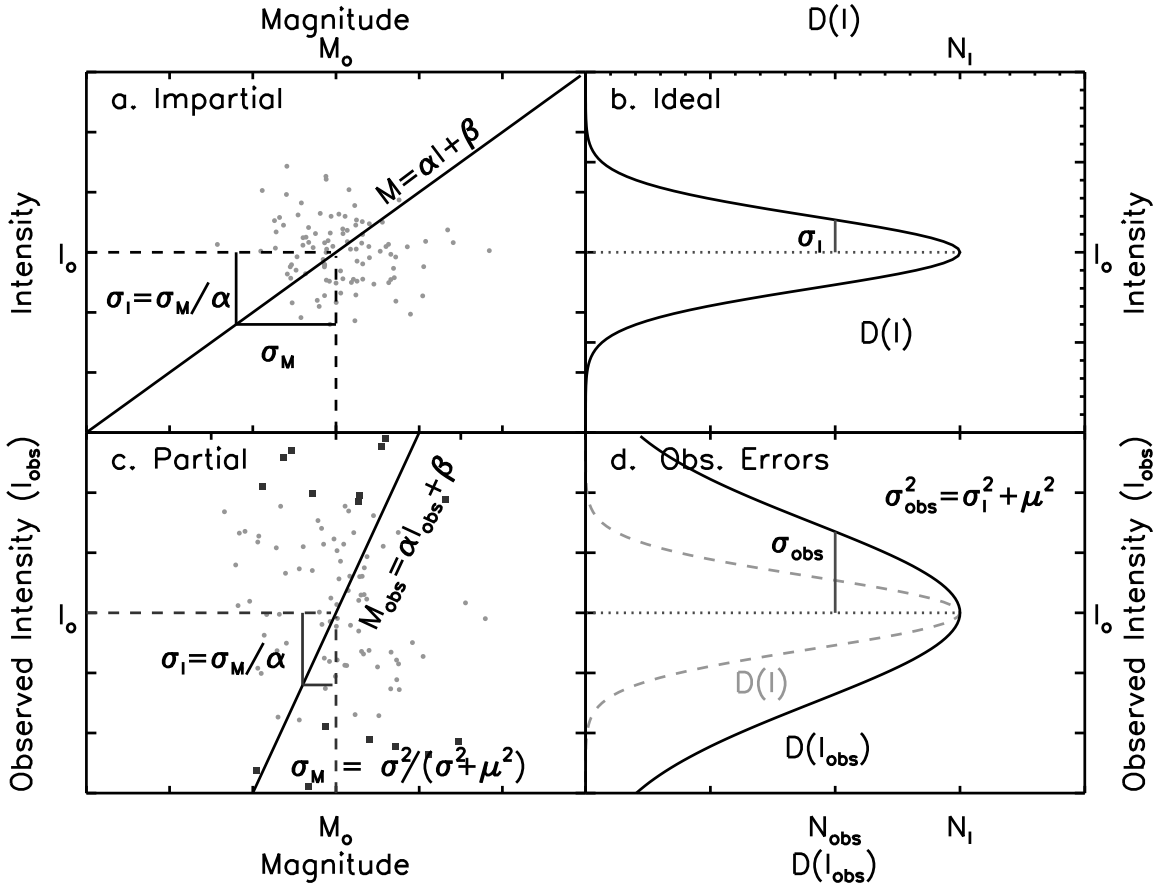

Fig. 9.— Demonstration of the impartial (*panels a and b*) and partial (*panels c and d*) calibration techniques for fictitious datasets without (i.e., "ideal") and with observational uncertainties, respectively. In the left panels, a fake dataset is drawn from the Gaussian distributions (filled circles) shown in the right panels; in both cases the black solid line represents the intrinsic spread, $D(I)$, of the data unconvolved with observational errors. For the case of the impartial calibration (*panels a and b*), all of the data drawn from the Gaussian distribution is used to derive the calibration line $M = \alpha I + \beta$ in *panel a*. For the case of the partial calibration, observational errors (presumed to be normally distributed with an RMS spread μ) inflate the observed spread of line intensities, $D(I_{obs})$ (*dashed curve*), but some measurements — the *black filled circles* in *panel c* — are rejected from the calibration sample as "extreme observational outliers". The spread of the remaining sample (it grey circles) mimics that of the intrinsic, error-free sample, $D(I)$ (*panel d*). However, the resulting calibration (*panel c*), $M_{obs} = \alpha I_{obs} + \beta$, is "torqued" with respect to that one would obtain from the error-free dataset (*panel a*). The actual quantitative differences are derived rigorously in Appendix B, following the discussion by Trumpler & Weaver (1953).

clustered around the visually identified mean value and this bias will have an effect magnitude distribution derived from the calibration. Moreover, there is a clear assumption in this procedure that the intrinsic variation within a given classification bin is small or at least well characterized by the calibration dataset (which was not the case). Stated differently, the Mount Wilson spectroscopists attributed the visible scatter entirely to uncertainties of an observational nature, which effectively ignores any "cosmic" or intrinsic variation (which could be larger or smaller than the observational scatter). In the case of A35, the Mount Wilson spectroscopists proceeded as if both steps, grouping and calibration within the group, were uncorrelated. This assumption produced both of the morphological differences between Figure 6b and Figure 6c: (i) the exaggerated separation between the luminosity classes, and (ii) the suppressed dispersion along each of the three sequences.

To illustrate the nature of the bias generated by this procedure, Figure 9 uses a pair of fictitious data sets to compare "impartial" and "partial" methods for which the grouping and calibration steps are uncorrelated and correlated, respectively. Figures 9a and 9b demonstrate the ideal or "impartial" calibration scenario, applied to an "error-free" dataset. In Figure 9a, we see the ideal calibration curve between absolute magnitude and line intensity derived from the distribution given in Figure 9b. In this case, intensity values (I) are selected by an "impartial" or independent means and the distribution of values, $D(I)$, and its intrinsic, cosmical spread, σ, are well sampled. Here the calibration utilizes the linear fit $M = \alpha I + \beta$ and the scale of the uncertainty in magnitudes, σ_M, follows the usual propagation, $\sigma_M = \alpha\sigma$. Our description here is analogous to the Blaauw (1963) discussion of "impartial" calibration of a dataset having no observational errors, but where the spread in line intensities is only given by a true intrinsic variation among a stellar type.

In Figure 9c the linear calibration fit resulting from a "partial" calibration is "torqued" or rotated from that derived in an "impartial" manner. The origin of this torque is the "partial" nature of the adopted line intensity groupings. The observed spread of line intensities in a sample where random observational errors are known to be convolving with the intrinsic line intensity spread, $D(I_{obs})$, there is a natural tendency to reject extreme outliers as being produced by the wings of the observational uncertainty distribution — presumed itself to be normally distributed with a dispersion μ — as a means to winnow the sample to one more representative of the error-free distribution, $D(I)$. However, the resulting fitted calibration, $M_{obs} = \alpha I_{obs} + \beta$ (based on those points shown in light gray, which fall in the distribution $D(I)$) not only has a steeper slope, but also a much smaller dispersion in M than would obtain in the error-free case (Figure 9). As shown in Appendix B, for the same line intensity spread, σ_i, the σ_M dispersion is reduced by a factor of $\sim 1/\sqrt{(}1 + \mu^2/\sigma^2)$ from the partial to the impartial analysis.

Thus, the effect of pursuing a "partial" calibration is not only an improper calibration relation for each relevant luminosity class, but the resulting range of magnitudes is also artificially compressed through the suppression of outliers. The former effect is evident in the comparison of M_{A35} to M_{HIP} in Figures 7a and 7b, in which the subgiant and giant branches appear "torqued" with respect to a one-to-one correlation, as well as in the compression of the subgiant and giant sequences in Figures 6b and 6c. Thus, the origin of the key differences in the A35 and *Hipparcos* CMDs lies in a subtle bias in the calibration technique used in A35.

Now, we can ask a different question: Though we have already shown that the subgiants in A35 are real, was their isolation in A35 a fortunate accident of this calibration error?

5.2.1. The Systematic Error

The "partial" nature of the A35 magnitude calibration curves was discussed at length in the literature of the time, most notably by Strömberg (1939), Strömberg (1940), Strömberg (1941), Russell & Moore (1938), Russell & Moore (1940), and van Rhijn (1939). These authors not only described the nature of the calibration bias, but also proceeded to correct the absolute magnitudes. The correction procedure relied on the existence of distances derived independent of A35, which are used to correct the "torque" shown in Figures 7a and 7b. A more detailed history of these papers and their efforts to correct the A35 catalog is given by Blaauw (1963), including more modern

use of the A35 catalog by Oke (1957, 1959) and Wilson & Vainu Bappu (1957).

While the "torque" correction method worked well for the dwarfs of all spectral types, application to the more distant subgiants and giants remained difficult owing to the smaller number of such stars having independently measured distances. As ground-based trigonometric samples grew, however, the correction method was applied to more giant type stars. For the A35 giants, however, the intensity line calibration method so torqued the axis (see the "squished" giant branch in Figure 6a), that the resulting corrections to A35 had large uncertainties. For the subgiants in Figure 6a, so compressed as to be completely detached from the main sequence and giant branches, correction of the A35 magnitudes was deemed impossible. An example calibration to spectral type K is given in Figure 5 of Blaauw (1963), to which Blaauw states, "With the accidental errors so strongly dominating the cosmic dispersion, it is obviously meaningless to try to introduce corrections to the Adams values for the giants. For the subgiants the situation is similar." Thus, the A35 data for the giants and subgiant classes were largely ignored owing to the inability to reconcile the bias introduced by the "partial" calibration.

It is important to note, that even at the time of Adrian Blaauw's 1963 summary article, only 41 K-giants and 12 K-subgiants had well measured trigonometric parallaxes — representing less than 10% of the total number of such stars in A35 (Blaauw 1963, S04). With the substantially larger *Hipparcos* database, 90% of the A35 stars now have independently measured parallaxes. In the next section, we endeavor to use these data to correct the full A35 HR diagram for the calibration bias to determine if the subgiants were created artificially by these biases.

5.2.2. Correcting for Systematic Errors in the Luminosity Calibration

In this subsection, we use the *Hipparcos* trigonometric parallaxes (Perryman et al. 1995; van Leeuwen 2007a,b, 2008) as a comparison sample to remove the torque in the A35 calibration curves (e.g., Figure 9c to 9a). First, we will describe the calibration method utilized by previous authors. Then, we will demonstrate its effectiveness for the G and K type stellar classes (i.e., those containing the majority of the subgiants in A35). Lastly, we apply the correction for all stars in A35 to revisit Figure 6 and create a corrected version of Figure 1 from A35. With this we aim to answer the question: if we remove the calibration torque in the A35 sample, do the 90 stars in A35 remain subgiants or do they largely join the main sequence or giant branches? Effectively, we ask whether the "partial" calibration method — the separation of stars into tightly concentrated fiducial values — artificially create the distinct, separated subgiant class?

To correct the A35 magnitudes using the *Hipparcos* sample, we transform our previous discussion into our set of variables specific to A35 and *Hipparcos*. Where possible, we follow the conventions used in the literature. We separate the sample by the A35 spectral type: A, F, G, K, and M, and then by luminosity class: dwarf, subgiant, and giant, using the A35 absolute magnitude. We first compute the mean magnitude for the spectral type and luminosity class in both the A35 sample, $\langle M_{A35} \rangle$, and the *Hipparcos* sample, $\langle M_{HIP} \rangle$, and define the difference between the two as,

$$\Delta\langle M \rangle = \langle M_{HIP} \rangle - \langle M_{A35} \rangle. \quad (1)$$

Then, we fit a linear regression for each luminosity class. The slope (m) of the fitted line represents the torque on the feature due to the improper calibrations (e.g, the relationship of Figure 9c). The quantity A, defined by Russell & Moore (1938) as the ratio of the dispersion of the measurement and the true dispersion is empirically derived by:

$$A = (1/m) - 1. \quad (2)$$

We then can compute the corrected magnitude for each star within a spectral and luminosity class using the following equation (Blaauw 1963, ; Equation 14):

$$M_{Corr} = M_{A35} + \Delta\langle M \rangle + A(M_{A35} + \Delta\langle M \rangle - \langle M_{HIP} \rangle) \quad (3)$$

where M_{Corr} is our final corrected A35 absolute magnitude, M_{A35} is the A35 absolute magnitude and, A is a quantity calculated from the results of the linear regression for a spectral and luminosity class and defined in Equation 2.

The process for correcting the magnitudes is demonstrated in Figure 10 for the A35 subgiant

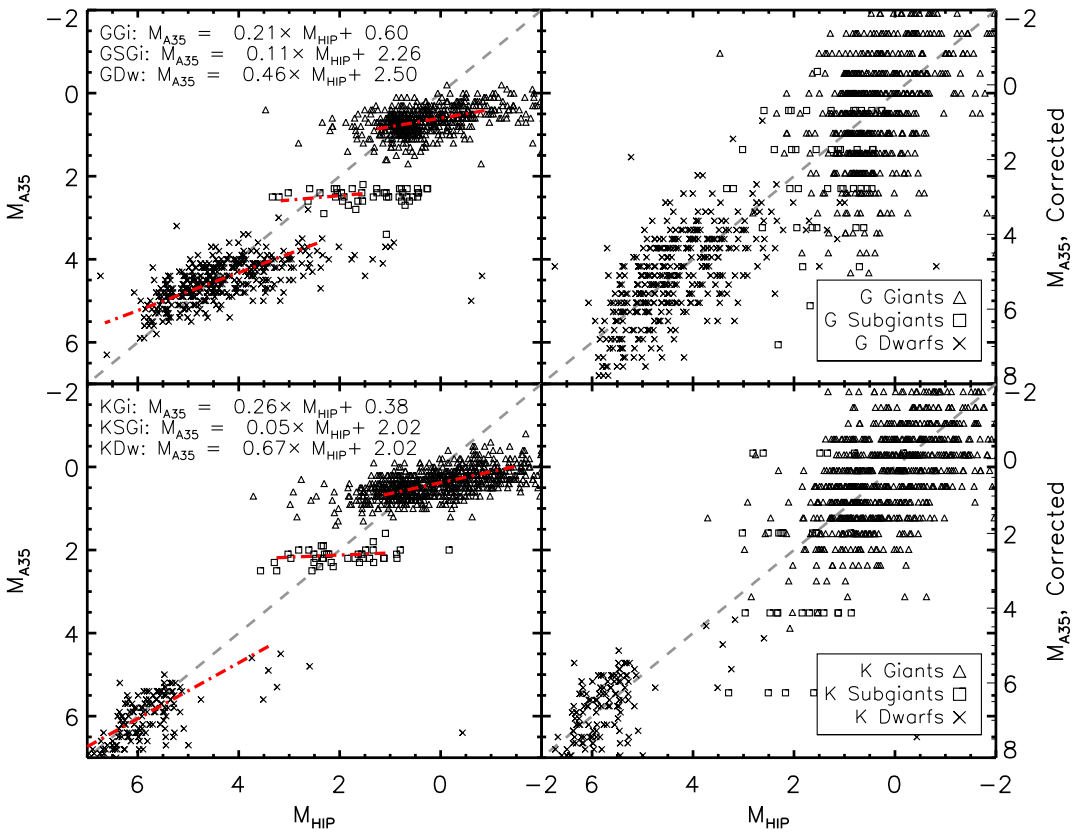

Fig. 10.— Procedure followed to calibrate the A35 magnitudes to the *Hipparcos* magnitudes following the detailed discussion in Blaauw (1963), and separated by G (*top*) and K (*bottom*) spectral types. The left panels display the original data with fits to the dwarfs (GDw, KDw), subgiants (GSGi, KSGi) and giants (GGi, KGi). We used the luminosity classifications in the *Hipparcos* catalog. In the right panels these calibration fits are applied to the A35 magnitudes and refit to demonstrate the removal of the torque.

spectral classes G (top panels) and K (bottom panels). In the left panels of Figure 10, the original A35 magnitudes are plotted against the corresponding *Hipparcos* magnitudes (M_{HIP}, as in Figure 7) — and illustrate the severe torque on the subgiant and giant luminosity calibrations in these classes. For each luminosity class, a linear regression is fit against those *Hipparcos* stars with σ_π/π less than 0.10 for the giants and less than 0.05 for the subgiants and dwarfs. The results of the linear regression are given in the left panels. In the right panels, the results of the fits are used in Equation 3 and applied to M_{A35}. In the right panels we accomplish both of the goals of this procedure: not only has the torque been corrected, but the observational scatter is increased to appropriate levels.

Having demonstrated that the larger *Hipparcos* database can correct the A35 magnitudes for the subgiants and giants, we proceed to use the *Hipparcos* data to correct the entire A35 sample and create the true HR diagram for the A35 sample. In Figure 11a the original A35 HR diagram is reproduced with the A35 spectral types color-coded in grayscale. In Figure 11b the corrected A35 magnitudes are plotted and the scatter within each of the luminosity and spectral type bins is greatly increased. In Figure 11c the *Hipparcos* HR diagram is shown with the same color scaling. Comparing Figures 11a, 11b, and 11c, it is clear that the correction procedure has recovered the true scatter appropriate to the A35 magnitudes, and this scatter is now larger than that of the modern, and more precise, magnitudes. Additionally, the subgiant sequence, shown in open boxes, is no longer detached from the main sequence or giant branch, instead a continuum of magnitudes is produced between these two phases of stellar evolution. In this modified version of the A35 diagram, the true transitionary nature of the subgiant sequences is revealed. Had it been realized at the time, it is possible that Gamow's conjecture might have been voiced more vociferously in scholarly circles, and potentially the ultimate understanding of stellar evolution would have been hastened.

6. Summary

1. The discovery of subgiants culminated with the summary paper by the Mount Wilson spectroscopists in 1935 that gave the absolute magnitudes of 4179 stars determined empirically from line ratios in their spectra that are sensitive to surface gravity.

2. The 90 Mount Wilson subgiant candidates formed a distinct sequence in the HR diagram between giant and dwarf stars and that was not attached either to the main sequence or to the giant sequence (Figure 6).

3. The problem posed at the 1957 Vatican Conference that high weight trigonometric parallaxes for a few field subgiants put them fainter than the subgiants in M67, believed then to be the oldest stars in the Galaxy (along with the globular clusters), was solved with the later discovery of the older Galactic clusters of NGC 188 and NGC 6791.

4. A test is made of the reality of the ∼90 stars that the Mount Wilson spectroscopists identified as part of the subgiant sequence via a star-by-star comparison of the Mount Wilson and the *Hipparcos* absolute magnitudes. A majority of the 90 Mount Wilson candidates that we have identified as the Adams et al. "subgiants" are clearly in the domain of subgiants when viewed in the modern *Hipparcos* color-magnitude diagram.

5. A strong correlation is found between the A35 spectroscopically derived absolute magnitudes for their subgiants and the corresponding absolute magnitudes for these stars derived using *Hipparcos* data. This statement holds even more broadly across all luminosity classes in the A35 database. We find for the subgiants that $\langle M_{V,\mathrm{MountWilson}} - M_{V,Hipparcos} \rangle = -0.12 \pm 0.02$ and with a dispersion of 1.02 magnitudes, when restricted to stars having *Hipparcos* $\sigma_\pi/\pi < 0.05$.

6. Tests for an observational selection incompleteness bias (e.g., the Malmquist bias) in the Strömberg (1930) calibration of the Mount Wilson subgiant sequence indicates that this bias did not artificially create the subgiant sequence in the A35 database as had been posited in the literature.

7. The reason for the narrow, disconnected A35 subgiant sequence is instead explained by a subtle bias in the A35 calibration curves that, while well known, could not be corrected for in the case of evolved stars due to the limited number of these stars in pre-*Hipparcos* trigonometric parallax samples. However, even after use of the *Hipparcos* parallaxes to correct for this historically well-

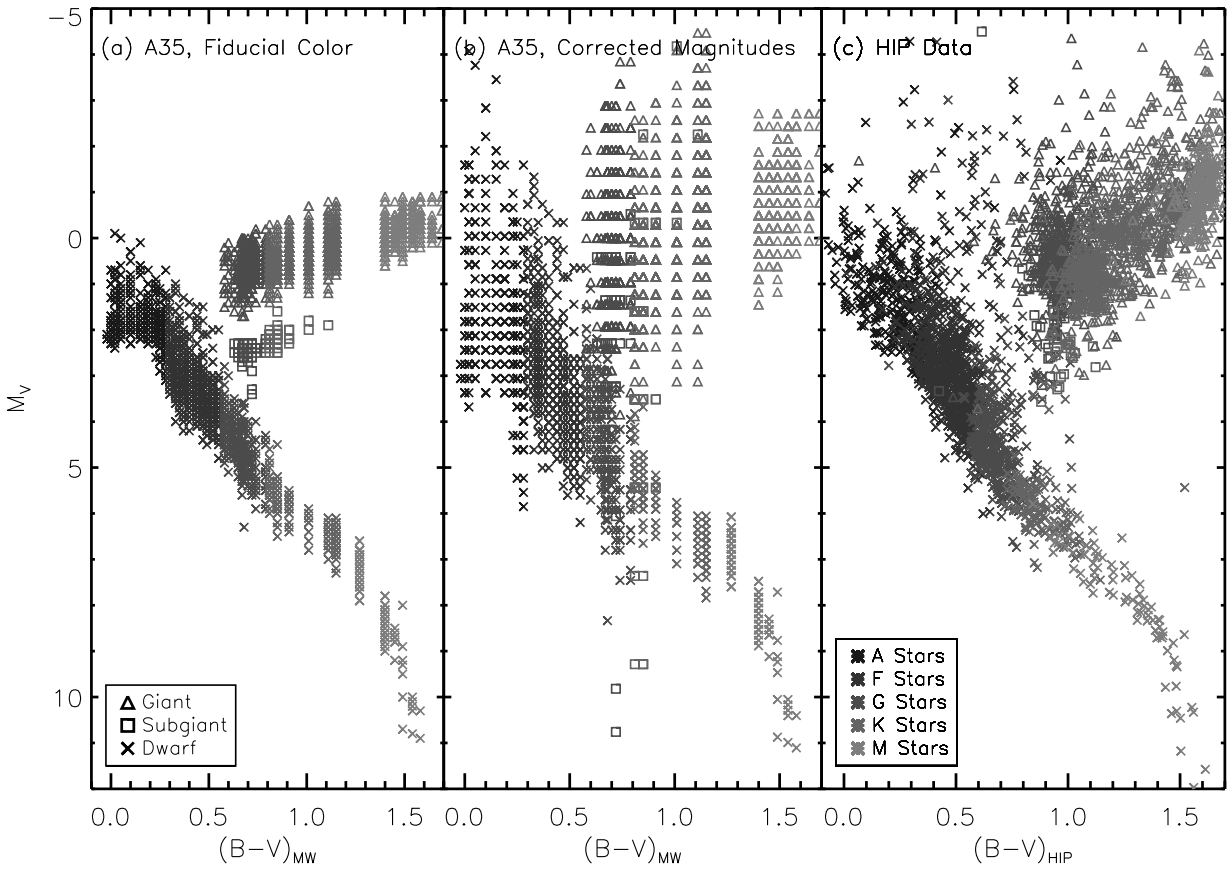

Fig. 11.— Application of the magnitude corrections to the A35 HR Diagram. In panel (a) we reproduce the A35 HR diagram with color axis translated from spectral types to a fiducial color. In panel (b) we apply the magnitude calibration procedure described in Section 5.2, and in panel (c) we reproduce the *Hipparcos* HR diagram for the A35 sample. Panel (b) demonstrates how correcting for the bias in the A35 methods brings visual impression of the A35 subgiants into better agreement with that of *Hipparcos*, most notably the subgiants now connect the main sequence and giant branch. The magnitude scatter along the sequences is now greater than that of *Hipparcos*.

discussed calibration bias we find that the A35 luminosity classes are robust and that the detection — and therefore discovery — of subgiants by the Mount Wilson spectroscopists is upheld.

7. A Note on the Preparation of this Manuscript

This work began as a collaboration between the authors in 2005 and progressed primarily by exchange of letters between AS and SRM until the death of AS in 2010. AS conceived the original concept and framework of the paper, and authored the original drafts of the manuscript. The historical insights described herein would not have been possible without AS's encyclopedic knowledge of, and indeed direct involvement in, many of the events described. Quantitative analyses and later stages in the crafting of the manuscript were carried on by RLB and SRM (in large part well after the passing of AS), and were only possible after intense study of pertinent writings of the numerous historical characters that played a role in the story described here. Special consideration was given to the handwritten letters, annotated drafts of the manuscript, and relevant published papers by AS himself so that we might attempt the closest fidelity of the final work to his original intent. Much as described by Sandage after the death of Edwin Hubble (albeit with far less significance of the product offered in the present paper!), RLB and SRM found themselves "lost in the shadow of a giant" in attempting to bring this work to the conclusion originally envisioned by the lead author. Much of his original outline and text has been preserved in this edition of the manuscript, but unfortunately we had to resort to our own less elegant prose in most of the later sections. AS is rightfully maintained as the primary author in that he was the originator and true leader of the project, but most especially to recognize his enthusiasm to rectify the historical judgment of the A35 work and to uphold the reputation of the Mount Wilson spectroscopists. This enthusiasm remained vibrant even as AS's health began to fail in 2008, and steadfast into his final months during which his production efficiency still well-outpaced that of his coauthors (who, at the time, were well behind in completing their contributions). An edited draft of the manuscript, with his sections already long completed, and a handwritten note signing off from the project due to declining health (dated August 7, 2010) were sent directly by AS via postal delivery and received by SRM two days after "Uncle Allan's" passing.

8. Acknowledgements

We wish to recognize helpful conversations with Richard Patterson and John Grula, as well as highly insightful comments from the anonymous referee that led us down a path to greatly improve this manuscript. RLB acknowledges assistance with OCR software from the Alderman Library Scholars Lab at the University of Virginia. Additionally, we acknowledge the encouragement from the family, friends and colleagues of AS, who also wished to see this work completed, including Mary Sandage, wife of the late Allan Sandage. RLB acknowledges support from the Jefferson Scholars Foundation as the C. Mark Pirrung Family Graduate Fellow in Astronomy and support from the Office of the Vice President of Research at the University of Virginia. RLB and SRM acknowledge support from NSF grants AST-0407207, AST-0807945 and AST-1109718.

A. APPENDIX A: Estimation of Lutz-Kelker Corrections

As briefly described in the main text, the Lutz-Kelker Effect (LKE, hereafter) is a bias that occurs due to the finite magnitude and sensitivity limits of trigonometric surveys. The scattering of stars in and out of the sample due to observational errors is asymmetric, more stars are scattered into the survey limits due to the larger volume element just outside of the survey than are scattered out from the volume element just inside. In this appendix, we supplement the brief discussion of the LKE in the main text by providing additional background on the LKE and a rigorous estimation of the appropriate offsets for the A35 catalog. As stated in the main text from a qualitative assessment, we find the LKE to be a very small effect for the A35 sample, especially when appropriately restricted by σ_π/π.

A.1. Background

Lutz & Kelker (1973) provided the first mathematical derivation of the Lutz-Kelker Effect (LKE), which had been alluded to in earlier work, in particular by Trumpler & Weaver (1953, but see Sandage & Saha (2002) for a detailed history of the bias). In this landmark paper, Lutz and Kelker found that the LKE was present for parallaxes independent of apparent magnitude and that it was best characterized by the dimensionless parameter, σ_π/π. The authors estimated the magnitude of the LKE as a function of $\sigma(\pi)/\pi$ for the case of a uniform stellar distribution ($P(\pi) \sim \pi^4$) for observations of stars with known intrinsic luminosity. Hanson (1979) derived a generalized form of the Lutz & Kelker derivation to other stellar distributions ($P(\pi) \sim \pi^n$), but still did not account for targeting bias in the trigonometric survey. Lutz (1979) expanded the results of Lutz & Kelker (1973) further and found two, as yet, unexplored complications for generalizing the LKE to other datasets. First, the intrinsic luminosity function of the sample must be known and *explicitly* included in the derivation of the Lutz-Kelker correction. Second, the behavior of the LKE with σ_π/π is more complex when an apparent magnitude (m_{app}) limit is imposed on the observational sample. Lutz (1979) highlights the most insidious aspect of the LKE; namely, that it has no general form. Instead, the appropriate Lutz-Kelker corrections must be derived independently for the specifications of a sample or even a subsample within a larger sample already characterized for LKE. We note that there is an on-going debate in the literature as to both the nature and applicability of this bias, in particular Smith (2003) and Francis (2014) present arguments for reconsidering the most common uses of the LKE.

A.2. Estimation of LKE for a General Sample

Sandage & Saha (2002, S02, hereafter) formalized the aforementioned complications into an easily adapted set of Monte-Carlo simulations that permits the calculation of Lutz-Kelker corrections for any trigonometric sample. This empirical approach is robust to concerns over the origin or functional form of the bias under debate in the literature. This work vividly illustrated the interplay of an m_{app} limit and the underlying stellar distribution in determining both the magnitude *and sign* of the Lutz-Kelker corrections. More specifically, their simulations revealed that the sign of the LKE can change across σ_π/π bins in a sample. In total, the complications explored by S02 emphasized the complexity of the bias and how its behavior is intrinsically unintuitive. To assess the role of the LKE on the *Hipparcos* absolute magnitudes matched to the A35 sample, we adapt the methodology of S02 to estimate the appropriate LKE corrections for the A35.

S02 was specifically focused on understanding the effect of the LKE on RR Lyrae stars, a class of stars typified by a narrow range of intrinsic luminosities. Our goal of understanding the effect of the LKE on the *Hipparcos* absolute magnitudes for the full A35 sample is more complicated due to the large range of intrinsic luminosities in the A35 sample. For the purposes of our calculation, we take the A35 absolute magnitudes to be the "true" intrinsic magnitude of the star. Then, we generate simulated datasets that we use to explore the LKE for A35.

To generate our simulated datasets, we populate a spherical volume of radius, $R = 400$ pc, assuming a model stellar distribution. This radius includes the majority of the A35 sample as was demonstrated in Figure 8. Stars are drawn from the A35 uniformly and, for full exploration of the bias, we repeatedly select stars until we have $N = 100,000$ stars. Each star is randomly assigned a distance within our volume drawn

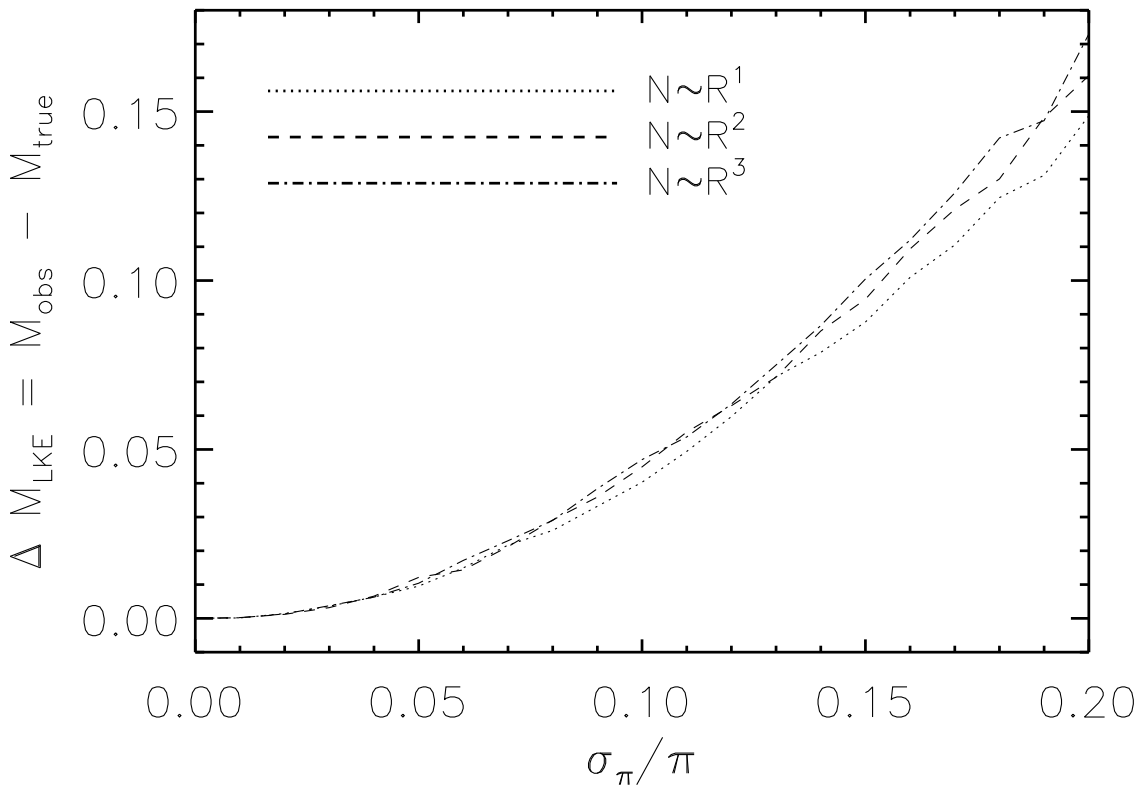

Fig. 12.— The Lutz-Kelker mean magnitude offset as a function of σ_π/σ. These values were derived by adapting the methodology of S02 to properties of the A35 sample. The offset is given for three assumed stellar distributions, $N \sim R^1, R^2, R^3$ in dotted, dashed and dot-dashed lines respectively. Over all the corrections for each stellar distribution track each other well in the A35 volume.

from the model distributions. This process is completed independently for each of the three model stellar distributions of S02, more specifically $N \sim R^n$ for $n = 1, 2, 3$. After placing the star in our volume, we compute apparent magnitude and the true parallax for each star, given its simulated distance. The true parallax is then given a random error drawn from a Gaussian distribution with width, $\sigma_\pi(m_{app})$. In a true parallax sample, this error will depend on the apparent magnitude of the star (m_{app}). To simulate the errors from the *Hipparcos* sample, we fit a linear relationship to the rms errors in the A35 sample, resulting in:

$$\sigma_\pi(m_{app}) = 0.07 * m_{app} + 0.431. \tag{A1}$$

This final parallax, the true parallax with an added error based on the apparent magnitude, is our simulated observed parallax for each star in our simulated sample.

Having calculated an observed parallax, we can compute the implied absolute magnitude for our simulated sample and compare it to the true magnitude used at the onset of the simulation. We calculate $\Delta M_{LKE} = M_{obs} - M_{true}$ for each star and compute the average value for the full sample as a function of σ_π/π.

The resulting Lutz-Kelker corrections are shown in Figure 12 as a function of σ_π/π for each of the stellar distributions, $N \sim R^n$ with $n = 0, 1, 2$. On the whole, these corrections are negligible for $\sigma_\pi/\pi < 0.05$. and, in general, are of the order of the errors typical of the A35 apparent magnitudes. For a more specific comparison, we give the corrections for the σ_π/π bins used for the paper in Table 2 for each of the stellar distributions. Thus, after proper consideration of the LKE, we conclude that it does not strongly influence our comparison of the A35 identified subgiants

B. APPENDIX B: HOW RANDOM ERRORS REDUCED SCATTER IN THE A35 MAGNITUDE CALIBRATIONS

In the main text, we presented a qualitative description of the bias introduced by the A35 spectroscopists by the due to choices in their calibration techniques. The bias creates two abnormal characteristics in the A35 color magnitude diagram (Figure 6a) as compared to the *Hipparcos* version (Figure 6c); these are: (i) compressed scatter along each luminosity sequence and (ii) enhanced separation between sequences in on the luminosity axis. We applied a correction procedure to correct for the bias, following the example of Russell & Moore (1938, 1940), and produce the A35 HR diagram with its true observational and intrinsic scatter. In supplement to the qualitative discussion given in the main text, we present a mathematical description of the bias in the A35 diagram due to the "impartial" calibration technique. This mathematical approach is based on the summary given by Blaauw (1963) of the various discussions from the literature (e.g., Strömberg 1939; Russell & Moore 1938, 1940) and is translated into the modern lexicon for the benefit of the reader.

In general, luminosity calibration occurs in two stages. First, a luminosity sensitive observable is identified, for A35 a set of spectral line intensities (I) correlated with stellar luminosity. Second, an empirical relationship is measured to map between the luminosity sensitive parameter and the absolute magnitude (M). To understand the origin of the systematic errors, we must consider how the magnitudes were calibrated.

B.1. The Ideal Case

First, we start with the ideal situation in which our line intensity distribution is well sampled by our observational data, meaning that the mean value (I_o) and dispersion (σ_{I_o}) calculated from the observational data are representative of their true, physical values. We start with a distribution of line intensities, $D(I)$, akin to the demonstration of Figure 9b in the main text. For simplicity, we assume that $D(I)$ is a Gaussian distribution, though the distribution could be any function. The mean value of the intensities is,

$$\langle D(I) \rangle = I_o \tag{B1}$$

with a dispersion of σ_I. We require that $D(I)$ is uniquely connected to a distribution of intrinsic magnitudes, $D(M)$.

Again, we assume that the desired magnitude (luminosity) distribution, $D(M)$, will also be Gaussian, such that the mean is given $\langle D(M)\rangle = M_o$ with a dispersion of σ_M. We further assume that the relation to connect $D(M)$ to $D(I)$ is unique, and, in imitation of the A35 calibration technique, that this relation is linear of the form:

$$M = \alpha I + \beta. \tag{B2}$$

By propagation of errors through Equation B2, errors in I (δI) translate to errors in M (δM) by

$$\delta M = \alpha \delta I. \tag{B3}$$

Likewise, the dispersion in M due to uncertainty in I is estimated by

$$\sigma_M = \alpha \sigma_I, \tag{B4}$$

and the mean magnitude of the resulting magnitude distribution $D(M)$ is determined by

$$M_o = \alpha I_o + \beta. \tag{B5}$$

We choose from our line intensity sample, $D(I)$, a subset with luminosity classifications from an independent technique, ideally absolute magnitudes determined from trigonometric parallaxes. The line intensity measurements (I) for this subsample will be observed to cluster narrowly around some central value, $I_1 \pm \Delta I$, and, ideally, this central value is I_o and the spread (ΔI) is given by σ_I (e.g., $I_1 = I_o$ and $\Delta I \approx \sigma_I$). For these stars we fit for α and β as described in Equation B1, and derive our set of absolute magnitudes ($D(M)$) with which we proceed to perform our science experiment. The mean values and dispersions of our absolute magnitude sample are computed directly from our line intensities following the relations given in Equations B3, B4, and B5, respectively.

This calibration case is deemed "impartial," because our line intensity data were grouped into calibration subsamples using a system "impartial" to the particulars of our observational systematics and uncertainties embedded within our line intensity distribution. Figure 13a is a visualization of this "ideal" scenario. A priori, we divide our distribution into luminosity classes (dwarf, subgiant, and giant) from the overall distribution and these classes, determined by an independent means, can be used to convert line intensities into absolute magnitudes for our full sample.

B.2. The Case of A35

In reality, however, our measurements are always imperfect due to (i) observational uncertainties and (ii) "cosmic uncertainties," (i.e. intrinsic star to star variation) both of which behave as sources of "random" uncertainty in our dataset. For sufficiently large sample sizes, these uncertainties can be minimized or, at least well characterized by the observational data itself (albeit they may not be readily distinguishable). *If* the the random uncertainties are well understood and appropriately characterized using independent datasets, then the case of calibration reduces to that of the "ideal".

In practice, these two independent types of error – observational (random) and cosmic — are indistinguishable without the acquisition additional data, and for our purpose here, we group them as a single, random error, μ_I. Now, we consider the effect of these, unrealized, random errors on the ideal case presented previously. This treatment is akin to that followed by the Mount Wilson spectroscopists for the absolute magnitudes presented in A35, and will demonstrate how incomplete consideration of random errors in the observational data, here $D(I)$, can produce reduced systematic errors in the resulting absolute magnitude distribution, $D(M)$.

For clarity, we redefine the line intensity distribution described previously, $D(I)$, to reflect observational error, $D(I_{obs})$. We assume it is Gaussian that can be described by $\langle D(I_{obs})\rangle = I_{o,obs}$ with scatter σ_{obs}, analogous to that case previously discussed. The mean value is not affected by random errors, so

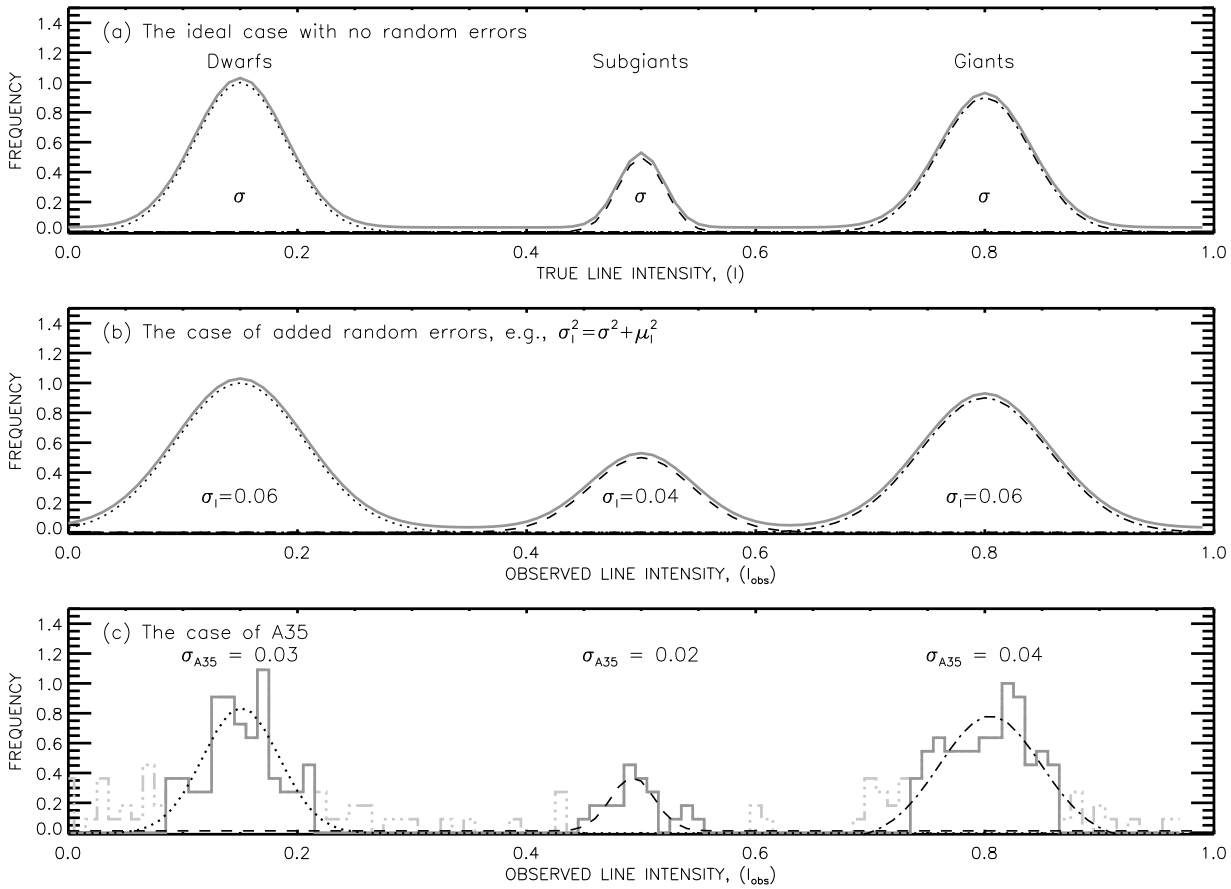

Fig. 13.— Schematic demonstration of the line intensity calibration scenarios described in the text. Each panel presents both a "total" distribution in thick grey, and the distribution for each of the three component luminosity classes in A35: dwarfs (dotted), subgiants (dashed), and giants (dot-dashed). In panel a, an "ideal" case is displayed with large samples of each class and no observational errors. Here each distribution is easily identified and distinguished for calibration. In panel b, a random error, μ, broadens each distribution, but the three distributions are still easily discriminated and their mean value is preserved. In panel c, we simulate the actual line intensity data of A35 by discretely sampling each of the luminosity class distributions (proportional to their representation in A35), and adding noise from a uniform distribution. In panel c, the light grey dot-dash distribution is the original sample, and the thick grey is the resulting sample after rejecting outliers and isolating the peaks. As in panel b, the mean value of each peak is preserved, but the resulting dispersion is suppressed from the outlier rejection. Though, we note that if all points (not just those passing the outlier rejection) are used in to fit each of the three distributions, then the true intrinsic dispersion is recovered.

$$\langle D(I)\rangle = \langle D(I_{obs})\rangle = I_o, \tag{B6}$$

as was given in Equation B1 for the ideal case. The scatter in our line intensity distribution ($D(I)$), however, increases such that the uncertainties add in quadrature, i.e.,

$$\sigma^2_{I,obs} = \sigma^2_I + \mu^2_I, \tag{B7}$$

where σ_I the scatter for the ideal case and μ_I is that from the observational uncertainty. This discussion is visualized in Figure 13b, in which the ideal distributions of Figure 13a are inflated with an additional random uncertainty, μ.

As before, we proceed to determine a relationship between $D(I)$ and $D(M)$ for physically motivated subsets of $D(I)$, the spectral and (ultimately) luminosity classes of the target stars. This is accomplished by selecting appropriate stars within a narrow range of some value $I_{1,obs} \pm \Delta I/2$ for each of our luminosity classes. Instead of grouping from an independent source as was done in the ideal case (Figure 13a), we instead plot a marginal distribution of all of our line intensities and identify peaks in the resulting distribution. This distribution is represented in Figure 13c by the dot-dash grey histogram, and we are able to identify the appropriate peaks, and their mean values, from this this distribution. We proceed to reject individual data points that seem distant from our mean values to isolate each distribution. The result of this process is shown in the grey thick line of Figure 13c. By following this method, we make an assumption (consciously or unconsciously) that the observed values do about some singular mean magnitude and that any scatter about that mean is completely driven by our observational errors. In turn, we suppress intrinsic variation within the class, or at the very least, assume it is smaller than our observational uncertainty. Using independent classification metrics would have alleviated this concern.

Thus, we have now restricted our observational data to a narrow range around a mean and these values no longer properly sample either the observed scatter (Figure 13b) *or* the true scatter (Figure 13a). Stars with large deviations from the mean intensities are removed under the assumption that they are not related to the true distribution of $D(I)$ (i.e., due to some observational error and not due intrinsic variation within the class), and, as demonstrated in Figure 13c, the resulting distributions are less broad. In this instance, our intuitive procedure for propagating error, $\delta M = \alpha \delta I$, is no longer valid within these highly constrained sub-samples Trumpler & Weaver (1953) and produces a constriction on the range of permissible values of I.

The true values I do not scatter symmetrically around the observed value $I_{1,obs}$. Following Trumpler & Weaver (1953, §1.51), for the case of "accidental" errors over a small range in a univariate distribution, the true mean value, $\langle I\rangle$, is described by:[8]

$$\langle I\rangle = I_{1,obs} + \frac{\mu^2_I}{D(I_{1,obs})}\frac{\delta D_{obs}}{\delta I_{obs}}(I_{1,obs}) + O(\mu^2_I) \tag{B8}$$

Where $O(\mu^2_I)$ represent terms of higher order in μ^2_I that are sufficiently small to ignore for our purposes.

Since $D(I_{obs})$ is a Gaussian distribution, it and its derivative can be substituted into Equation A8, such that, with rearrangement, we obtain[9]:

$$\langle I\rangle = I_{1,obs} - (I_{1,obs} - I_o) \times \frac{\mu^2_I}{\sigma^2_{I,obs}}. \tag{B9}$$

With additional rearrangement, we obtain a form that better elucidates the systematic error between the true and the observed mean values:

[8]The equation A8 comes from §1.51 *Correction of a univariate distribution for observational errors* for the case of *Average errors for small intervals of the measured values* of Trumpler & Weaver (1953).

[9]This relation deviates slightly from the precursor to Equation 7 in Blaauw (1963) due to what we suspect to be a typographical error in that text.

$$\frac{\sigma_I^2 + \mu_I^2}{\sigma_I^2} = \frac{(I_{1,obs} - I_o)}{(\langle I \rangle - I_o)} \tag{B10}$$

First, we note that the previous equation is the ratio of the relations, $(\langle I \rangle - I_o)$ and $(I_{1,obs} - I_o)$ are, effectively, divisions on the true and observed intensity axis scales about the mean, respectively. Second, the ratio of the true and observed axes is independent of the actual observed values (I_{obs}). Third, Equation B10 is always less than unity, as the observational uncertainty is always larger than zero ($\mu_I > 0$).

Now, we again fit a relationship to calibrate our subset, deriving: $\langle M \rangle = \alpha \langle I \rangle + \beta$. Though similar in form, this is *not* equivalent to the relationship derived earlier for our idealized case, $M_o = \alpha I_o + \beta$. Here, when we derive our calibration curve, we compare $\langle M \rangle$ against the measured value, $\langle I_{obs} \rangle$, and not its true value, I_o. Effectively, as was demonstrated for $D(I_{obs})$ in Equation B10, we measure our relation on an axis that is compressed by improper treatment of the observational uncertainty, and this compression is propagated into the resulting distribution of absolute magnitudes $D(M_{obs})$. As demonstrated by Figure 9 in the main text, the resulting calibration curves are "torqued" resulting in a narrower output distribution than is reasonable for the input observational data.

Our derived values ($D(M_{obs})$) are also compressed compared to the true distribution $D(M)$. There are two factors to consider in estimating the degree of compression in $D(M_{obs})$. First, we know that the observed dispersion is greater than the true dispersion by a factor of $\sigma_{I,obs}/\sigma_I$, e.g. going from Figure 13a and Figure 13b. Second, the effective range of intensities is compressed by our outlier rejection by $\sigma_I^2/(\sigma_I^2 + \mu_I^2)$, e.g., the transition from Figure 13b and Figure 13c. Combining the two factors, we arrive at the ratio of the true dispersion (σ) to the final dispersion of absolute magnitudes (σ_{A35}):

$$\frac{\sigma_{A35}}{\sigma} = \frac{\sigma_{I,obs}}{\sigma_I} \times \frac{\sigma_I^2}{(\sigma_I^2 + \mu_I^2)} \tag{B11}$$

Substituting for $\sigma_{I,obs}$ from Equation B7, we obtain a final expression relating the A35 dispersion to the true dispersion and random errors:

$$\sigma_{A35} = \frac{\alpha\sigma}{\sqrt{1 + \mu_I^2/\sigma_I^2}} \tag{B12}$$

The denominator, $\sqrt{1 + \mu_I^2/\sigma_I^2}$, is always greater than unity, and σ_{A35} will, therefore, be smaller than the true dispersion (σ) of the luminosity class. Perhaps against our intuition, the resulting random errors in $D(M)$ are not increased by an amount proportional to the uncertainty in the line intensities, but are instead compressed by this observational error. Effectively, by removing outliers without insight from a means independent of our input data, we compress the effective output range of our absolute magnitude calibration. The compression in the output range explains both of the morphological concerns regarding the the shape and separation of the luminosity classes in the A35 CMD (Figure 6a).

REFERENCES

Adams, W. S. 1916a, Proceedings of the National Academy of Science, 2, 143

—. 1916b, Proceedings of the National Academy of Science, 2, 147

—. 1916c, Proceedings of the National Academy of Science, 2, 152

—. 1916d, Proceedings of the National Academy of Science, 2, 157

—. 1929, PASP, 41, 195

—. 1933, PASP, 45, 215

Adams, W. S., & Joy, A. H. 1917, ApJ, 46, 313

Adams, W. S., & Joy, A. H. 1922, in Publications of the American Astronomical Society, Vol. 4, Publications of the American Astronomical Society, 201

Adams, W. S., Joy, A. H., & Humason, M. L. 1926, ApJ, 64, 225

Adams, W. S., Joy, A. H., Humason, M. L., & Brayton, A. M. 1935, ApJ, 81, 187

Adams, W. S., Joy, A. H., Stromberg, G., & Burwell, C. G. 1921, ApJ, 53, 13

Adams, W. S., & Kohlschütter, A. 1914, ApJ, 40, 385

Adams, W. S., & Russell, H. N. 1928, ApJ, 68, 9

Baade, W. 1958, Ricerche Astronomiche, 5, 303

Blaauw, A. 1963, The Calibration of Luminosity Criteria, ed. K. A. Strand (the University of Chicago Press), 383

—. 2004, ARA&A, 42, 1

Brown, A. G. A., Arenou, F., van Leeuwen, F., Lindegren, L., & Luri, X. 1998, Highlights of Astronomy, 11, 547

Chaboyer, B., Green, E. M., & Liebert, J. 1999, AJ, 117, 1360

Curtis, H. D. 1922, PASP, 34, 33

DeVorkin, D. H. 2006, Journal for the History of Astronomy, 37, 429

Eggen, O. 1957, AJ, 62, 45

Eggen, O. J. 1955, PASP, 67, 315

—. 1960, MNRAS, 120, 430

—. 1964, AJ, 69, 570

Francis, C. 2014, MNRAS, 444, L6

Gray, R. O., & Corbally, J., C. 2009, Stellar Spectral Classification

Hanson, R. B. 1979, MNRAS, 186, 875

Hertzsprung, E. 1905, Zeitschrift Fur Wissenschaftliche Photographie, 3, 442

—. 1907, Zeitschrift Fur Wissenschaftliche Photographie, 5, 86

Jaschek, C., & Gomez, A. E. 1998, A&A, 330, 619

Johnson, H. L. 1954, ApJ, 120, 325

—. 1966, ARA&A, 4, 193

Johnson, H. L., & Sandage, A. R. 1955, ApJ, 121, 616

Kaluzny, J., & Rucinski, S. M. 1995, A&AS, 114, 1

Kinman, T. D. 1965, ApJ, 142, 655

Kovalevsky, J. 1998, ARA&A, 36, 99

Lundmark, K. 1932, Handbuch der Astrophysik, 5, 210

Lutz, T. E. 1979, MNRAS, 189, 273

Lutz, T. E., & Kelker, D. H. 1973, PASP, 85, 573

Luyten, W. J. 1922, Lick Observatory Bulletin, 10, 135

Morgan, W. W. 1937, ApJ, 85, 380

Morgan, W. W., Keenan, P. C., & Kellman, E. 1943, An atlas of stellar spectra, with an outline of spectral classification

O'Connell, D. J. K. 1958, Ricerche Astronomiche, 5

Oke, J. B. 1957, ApJ, 126, 509

—. 1959, ApJ, 130, 487

Oudmaijer, R. D., Groenewegen, M. A. T., & Schrijver, H. 1998, MNRAS, 294, L41

Perryman, M. A. C., Lindegren, L., Kovalevsky, J., et al. 1995, A&A, 304, 69

Russell, H. N. 1914, Popular Astronomy, 22, 331

—. 1925a, Scientific American, 133, 241

—. 1925b, Nature, 116, 209

Russell, H. N., & Moore, C. E. 1938, ApJ, 87, 389

—. 1940, ApJ, 92, 354

Saha, M. N. 1921, Royal Society of London Proceedings Series A, 99, 135

Sandage, A. 1958a, Ricerche Astronomiche, 5, 41

—. 1958b, Ricerche Astronomiche, 5, 287

—. 1962, ApJ, 135, 333

—. 1986, ARA&A, 24, 421

—. 2001, The Malmquist Bias, ed. P. Murdin (Taylor & Francis, Boca Raton)

—. 2004, Centennial History of the Carnegie Institution of Washington, Vol.I; The Mount Wilson Observatory (Cambridge Univ. Cambridge Press)

Sandage, A., Lubin, L. M., & VandenBerg, D. A. 2003, PASP, 115, 1187

Sandage, A., & Saha, A. 2002, AJ, 123, 2047

Sandage, A. R., & Eggen, O. J. 1959, MNRAS, 119, 278

Schmidt-Kaler, T. 1982, Landolt-Börnstein: Numerical Data and Funcational Relationshipsin Science and Technology, ed. K. Schaifers & H. Voigt (Berlin, Springer-Verlag)

Smith, H. 2003, MNRAS, 338, 891

Strömberg, G. 1930, ApJ, 71, 175

—. 1932, ApJ, 75, 115

—. 1936, ApJ, 84, 412

—. 1939, ApJ, 89, 10

—. 1940, ApJ, 92, 156

—. 1941, ApJ, 93, 33

ten Bruggencate, P. 1927, Sternhaufen: Ihr Bau, Ihre Stellung zum Sternsystem und Ihre Bedeutung für die Kosmogonie

Trumpler, R. J., & Weaver, H. F. 1953, Statistical astronomy

van Leeuwen, F., ed. 2007a, Astrophysics and Space Science Library, Vol. 350, Hipparcos, the New Reduction of the Raw Data

van Leeuwen, F. 2007b, A&A, 474, 653

—. 2008, VizieR Online Data Catalog, 1311, 0

van Rhijn, P. J. 1939, Publications of the Kapteyn Astronomical Laboratory Groningen, 49, 1

Wilson, O. C., & Vainu Bappu, M. K. 1957, ApJ, 125, 661

This 2-column preprint was prepared with the AAS LaTeX macros v5.2.

TABLE 1

DATA FOR THE 90 MOUNT WILSON SUBGIANTS THAT FROM THEIR SPECTRA DEFINED THE CLASS IN 1935

Star Name Mt. W.	Star Name Hip.	*Hipparcos* V	*Hipparcos* $B-V$	Sp.Type Mt. W.	Sp.Type Hip.	π (mas) Mt. W.	π (mas) Hip.	$\sigma(\pi)/\pi$ Hip.	$M_V(\pi)$ Mt. W.	$M_V(\pi)$ Hip.
HD 28	HIP 443	4.61	1.03	K0	K1 III	20	25.38	0.04	2.1	1.63
HD 1037	HIP 1176	6.63	1.03	G8	G8 III/IV	13	7.76	0.10	2.4	1.08
HD 2589	HIP 2242	6.18	0.88	G9	K0 IV	17	25.37	0.02	2.5	3.20
HD 3546	HIP 3031	4.34	0.87	G3	G5 III	42	19.34	0.04	2.6	0.77
HD 4398	HIP 3607	5.49	0.98	G6	G8/K0 III	23	9.78	0.07	2.4	0.44
HD 5268	HIP 4257	6.15	0.91	G3	G5 IV	17	8.60	0.09	2.5	0.82
HD 5286	HIP 4288	5.46	1.01	K1	K1 IV	17	25.69	0.05	2.3	2.51
HD 5395	HIP 4422	4.62	0.96	G4	G8 III/IV	36	15.84	0.04	2.6	0.62
HD 6473	HIP 5412	6.24	0.92	G6	K0	17	6.97	0.08	2.5	0.46
HD 8512	HIP 6537	3.60	1.07	K0	KO III	46	28.48	0.03	2.1	0.87
HD 10486	HIP 8044	6.33	1.02	K2	K2 IV	13	18.04	0.04	2.0	2.61
HD 16042	HIP 12053	8.24	1.07	G4	K0 V	6	4.02	0.28	2.4	1.26
HD 20618	HIP 15514	5.91	0.86	G5	G8 IV	21	15.88	0.07	2.5	1.91
HD 21467	HIP 16181	6.03	0.95	G6	KO IV	21	14.44	0.06	2.7	1.83
HD 29613	HIP 21685	5.46	1.05	K1	K0 III	21	16.42	0.04	2.2	1.54
HD 34538	HIP 24679	5.48	0.93	G9	G8 IV	21	20.69	0.04	2.3	2.06
HD 34642	HIP 24659	4.81	0.99	K0	K0/K1 III/IV	30	29.63	0.02	2.3	2.17
HD 37160	HIP 26466	4.09	0.95	G6	G8 III/IV	42	28.10	0.03	2.5	1.33
HD 37601	HIP 26941	6.05	0.95	G9	K0 III	17	16.26	0.04	2.3	2.11
HD 37981	HIP 26930	6.72	1.10	K1	K1 IV	10	8.98	0.11	2.0	1.49
HD 39169	HIP 27600	7.85	1.06	K0	G5	7	5.52	0.43	2.1	1.56
HD 39364	HIP 27654	3.76	0.98	G7	G8 III/IV	79	29.05	0.02	3.4	1.08
HD 40959	...	...	...	G5	...	5	...	...	2.4	...
HD 45410	HIP 31039	5.86	0.93	G8	K0 IV	20	17.56	0.04	2.5	2.08
HD 46480	HIP 31676	5.94	0.90	G7	G8 IV/V	24	18.82	0.04	2.9	2.31
HD 55280	HIP 35146	5.20	1.08	K2	K2 III	22	16.88	0.05	2.0	1.34
HD 71952	HIP 41894	6.23	1.01	K0	K0 IV	14	16.65	0.04	2.2	2.34
HD 73593	HIP 42604	5.35	0.99	G6	G0 IV	26	18.11	0.04	2.6	1.64
HD 75558	HIP 43463	7.38	0.91	G3	G5	11	5.37	0.20	2.5	1.03
HD 77818	HIP 44766	7.62	1.00	K0	K1 IV	8	8.72	0.10	2.2	2.32
HD 78249	HIP 44990	7.07	0.98	K2	K1 IV	10	15.11	0.05	2.2	2.97
HD 79452	HIP 45412	5.98	0.84	G3	G6 III	18	7.17	0.13	2.3	0.26
HD 84406	HIP 48034	6.94	0.95	K0	G5	13	13.24	0.05	2.5	2.55
HD 84453	HIP 47973	6.81	0.95	K0	K0 IV	11	12.06	0.07	2.1	2.22
HD 86359	HIP 48881	7.45	0.92	G7	G5	9	10.69	0.10	2.3	2.59
HD 90752	HIP 51204	7.23	0.97	G9	K0	9	7.27	0.20	2.2	1.54
HD 91011	HIP 51451	6.98	1.03	K0	K0	10	6.76	0.15	2.2	1.13
HD 92588	HIP 52316	6.25	0.88	K1	K1 IV	17	29.08	0.03	2.5	3.57
HD 93636	HIP 52882	6.15	1.14	K1	K0	14	5.45	0.14	2.0	-0.17
HD 94178	HIP 53179	7.52	0.91	G7	G5	9	9.41	0.11	2.4	2.39
HD 94264	HIP 53229	3.79	1.04	K2	K0 III/IV	46	33.40	0.02	2.2	1.41
HD 96074	HIP 54275	7.65	0.93	G8	G5	9	6.06	0.13	2.4	1.56
HD 96436	HIP 54336	5.52	0.96	G7	G9 IIICN	24	16.05	0.06	2.6	1.55
HD 97100	...	...	...	G5	...	5	...	...	2.5	...
HD 102928	HIP 57791	5.62	1.06	K0	K0 IV	17	12.59	0.08	2.2	1.12
HD 105639	HIP 59285	5.95	1.12	K3	K3 III	14	11.94	0.07	1.8	1.34
HD 110646	HIP 62103	5.91	0.85	G4	G8 IIIp	22	14.26	0.05	2.8	1.68
HD 111028	HIP 62325	5.65	0.99	K1	K1 III/IV	20	22.36	0.04	2.4	2.40
HD 113817	HIP 63960	7.09	0.98	G8	K0 III	11	4.67	0.20	2.4	0.44
HD 115202	HIP 64725	5.21	1.01	K1	K1 III	23	25.68	0.03	2.1	2.26
HD 116713	HIP 65535	5.11	1.18	K1	Kp	19	15.73	0.05	1.6	1.09
HD 123409	HIP 68955	6.89	1.00	G6	K0	13	5.71	0.14	2.5	0.67
HD 126400	HIP 70538	6.48	0.94	G7	K0 III	14	12.99	0.08	2.4	2.05
HD 127243	HIP 70791	5.58	0.86	G4	G3 IV	26	10.59	0.06	2.7	0.70
HD 138716	HIP 76219	4.61	1.00	K1	K1 IV	29	34.54	0.02	2.1	2.30
HD 140301	HIP 77007	6.30	1.12	K0	K0 III	13	7.94	0.11	2.0	0.80
HD 140687	...	...	...	K1	...	9	...	...	2.3	...
HD 142091	HIP 77655	4.79	1.00	K1	K0 III/IV	26	32.13	0.02	1.9	2.32
HD 143586	...	...	...	G9	...	5	...	...	2.3	...
HD 150275	HIP 80850	6.35	1.00	K0	K1 III	14	8.00	0.07	2.2	0.87
HD 151216	HIP 81977	9.17	1.03	K1	K2	4	3.20	0.36	2.2	1.70
HD 152781	HIP 82861	6.33	0.95	K2	K0/K1 III/IV	14	24.72	0.03	2.3	3.30
ADS 10394B	...	...	...	K0	...	5	...	...	1.8	...
HD 156461	HIP 84647	7.23	1.02	G3	G8 III	11	5.86	0.20	2.5	1.07
HD 159466	HIP 85979	6.52	0.95	G4	G8 III	14	6.40	0.15	2.5	0.55
HD 160042	HIP 86352	6.19	0.83	G7	G6 III/IV	14	9.66	0.09	2.4	1.11
HD 162076	HIP 87158	5.69	0.94	G5	G5 IV	20	13.04	0.05	2.3	1.27
HD 165438	HIP 88684	5.74	0.97	K1	K1 IV	17	28.61	0.03	2.1	3.02
HD 167042	HIP 89047	5.97	0.94	K0	K1 III	18	20.00	0.03	2.2	2.48
HD 173399	HIP 91782	8.99	0.42	G2	F2 V	12	7.39	0.89	2.5	3.33
HD 173949	HIP 91915	6.02	0.97	G7	G7 IV	16	8.95	0.06	2.3	0.78
HD 181391	HIP 95066	4.98	0.94	K0	G8 III/IV	24	21.17	0.04	2.3	1.61
HD 185351	HIP 96459	5.17	0.93	K0	K0 III	27	24.64	0.02	2.4	2.13
HD 194433	HIP 100852	6.24	0.96	K1	K1 IV	17	25.21	0.05	2.5	3.25
HD 196925	HIP 101082	5.96	0.94	G8	K0 III+	18	15.88	0.03	2.4	1.96
HD 198149	HIP 102422	3.41	0.91	G7	K0 IV	63	69.73	0.01	2.6	2.63
HD 198732	HIP 103071	6.32	0.88	G5	K0 III	19	13.33	0.09	2.6	1.94
HD 198896	HIP 102990	7.91	0.62	G7	Am	9	0.33	6.55	3.3	-4.50
HD 199223	HIP 103301	6.04	0.82	G6	G6 III/IV	17	9.02	0.13	2.3	0.82
HD 200004	HIP 103728	6.55	0.85	G3	G6/G8 III	14	6.05	0.16	2.3	0.46
HD 202403	HIP 104844	7.08	0.80	G5	G5	8	5.21	0.23	2.3	0.66
BD +15 466	...	...	...	K3	...	4	...	...	2.1	...
HD 212943	HIP 110680	4.78	1.04	K0	K0 III	30	20.39	0.04	2.3	1.33
HD 216640	HIP 113148	5.53	1.11	K4	K1 III	17	23.27	0.03	1.9	2.36
HD 218527	HIP 114273	5.42	0.91	G4	G8 IV	23	11.64	0.11	2.4	0.75

TABLE 1—*Continued*

Star Name Mt. W.	Star Name Hip.	*Hipparcos* V	*Hipparcos* $B-V$	Sp.Type Mt. W.	Sp.Type Hip.	π (mas) Mt. W.	π (mas) Hip.	$\sigma(\pi)/\pi$ Hip.	$M_V(\pi)$ Mt. W.	$M_V(\pi)$ Hip.
HD 221148	HIP 115953	6.26	1.12	K3	K3 IIIvar	13	20.44	0.04	2.0	2.81
HD 221639	HIP 116251	7.20	0.92	G9	K1 V	10	14.58	0.05	2.4	3.02
HD 222107	HIP 116584	3.81	0.98	G7	G8 III/IV	40	38.74	0.02	2.3	1.75
HD 222404	HIP 116727	3.21	1.03	K1	K1 IV	55	72.50	0.01	2.1	2.51

TABLE 2
LUTZ-KELKER CORRECTIONS FOR A35 SAMPLE

σ_π/π	$N \sim R^1$ ΔM_{LKE}	$N \sim R^2$ ΔM_{LKE}	$N \sim R^3$ ΔM_{LKE}
0.01	0.000	0.000	0.000
0.05	0.095	0.012	0.010
0.10	0.040	0.045	0.047
0.15	0.088	0.094	0.100
0.20	0.149	0.161	0.173
0.25	0.205	0.222	0.241

This figure "f2.png" is available in "png" format from:

http://arxiv.org/ps/1511.05930v1

This figure "f5_small.png" is available in "png" format from:

http://arxiv.org/ps/1511.05930v1